Predictive Control Strategies for Automotive Engine Coldstart Emissions

by

Ahmad Mozaffari

A thesis
presented to the University of Waterloo
in fulfillment of the
thesis requirement for the degree of
Master of Applied Science
in
Systems Design Engineering

Waterloo, Ontario, Canada, 2015

Author's Declaration

I hereby declare that I am the sole author of this thesis. This is a true copy of the thesis, including any required final revisions, as accepted by my examiners.

I understand that my thesis may be made electronically available to the public.

Abstract

In this study, a comprehensive investigation is carried out to study the effectiveness of model-based predictive control strategies to solve a formidable automotive control problem, that is, reducing the amount of cumulative hydrocarbon (*HC)* tailpipe emissions or HC_{cum} over the first few minutes of an automotive engine operation which is known as the coldstart period. More than 80% of the total *HC* emissions for a typical driving cycle are generated during the coldstart period. There is a physical trade-off between increasing the exhaust gas temperature (T_{exh}) and reducing engine-out hydrocarbon emission ($HC_{raw\text{-}c}$), which are two key variables affecting the engine performance during the coldstart operation. The design of an effective coldstart controller is associated with lots of difficulties because the behavior of the engine in the coldstart period is highly transient, uncertain, and nonlinear, and also, the key factors are in confliction with each other.

In the light of promising reports on the performance of model predictive controllers (MPCs), here, different variants of MPCs are taken into account to find out whether they can effectively cope with the difficulties associated with the coldstart problem for a given automotive engine. The major advantage of MPCs refers to their power to handle different constraints while trying to minimize an objective function to come up with optimal controlling signals. Other than the standard version of MPCs, in this work, some novel versions of such controllers are proposed, which are best suited for the considered control problem. The considered versions of MPCs are: nonlinear MPC (NMPC), preference-based model predictive controller (PBNMPC), and receding horizon sliding controller (RHSC). Also, a powerful classical optimal controller based on the Pontryagin's minimum principle (PMP) is taken into account to ascertain the veracity of the considered predictive controlling methods. Through an exhaustive simulation, the efficacy of proposed predictive controlling techniques is demonstrated, and also, it is indicated how well such controllers can optimize the related objective function at the heart of coldstart control problem while handling a set of the operating constraints.

Acknowledgements

I would like to thank my supervisor, Professor Nasser L. Azad, for his support and guidance, and also Professor Karl Hedrick and Andreas Hansen from University of California Berkeley, for their valuable feedback on the devised coldstart controllers. I am also grateful to Professor Shoja Chenouri and Professor Andrea Scott for providing constructive and valuable comments on my thesis.

Table of Contents

List of Figures

List of Tables

Chapter 1

Introduction

1.1 Background

Over the past decades, an astonishing trend has emerged towards developing effective controllers to improve the performance of vehicles [1]. The main reason for this phenomenon lies in the fact that enhancing the performance of automobiles by means of designing and implementing more advanced controllers is much more cost-effective compared to devising and applying new hardware for them. In particular, it has been demonstrated that applying optimal controlling algorithms can significantly decrease the fuel consumption and emissions of vehicle systems without any additional costs for replacing or modifying any other part of the vehicle. In this way, a proper controller can be designed to improve different aspects of automotive engines as one of the most important components of the vehicle. For improving the performance of a given engine, several operating metrics can be defined which focus on advancing specific characteristics of the engine, and thus, certain controllers with pre-defined goals can be designed to enhance each of those features. To use a new controller for improving the vehicle's engine performance, it is only required to implement the new control algorithm (written in a certain programming environment) on the related electronic control unit (ECU) and apply it to regulate the engine functioning during a driving cycle [2].

After lots of experiments and analyses by automotive engineers and researchers, nowadays, there is a wide consensus on the above-mentioned claim about vehicle control systems, and there has been an increasing interest among the automotive research community to come up with advanced controlling strategies to be used at the hearts of vehicle systems' ECUs to enhance their performance [3]. By investigating the archived literature on designing controllers for automobiles, it can be inferred that the main focus of these studies has been on developing control systems for reducing the amount of emissions [4], decreasing fuel consumptions [5], decreasing travel times [6], and increasing the safety of vehicle motions [7] during the driving

period. Various types of offline, online, model-based, and heuristic controllers have been designed so far to comply with the above-mentioned objectives. Among the existing controllers, those implemented based on the concept of Pontryagin's minimum principle (PMP) [8], model predictive control (MPC) [9], fuzzy theory [10], linear quadratic tracking system (LQTS) [11], sliding mode control (SMC) [12], neural controlling systems [13], switching hybrid control system (SHCS) [14], game theoretic-based controllers [15], robust state feedback stabilization controller [16], and dynamic programming (DP) [17] have been proven to show the most promising results. However, the research on designing more advanced vehicle controllers is still an open area of investigation, and researchers are trying very hard to take advantage from advanced mathematics-based and computational intelligence-based tools to increase the effectiveness of the current controllers [18].

Arguably, among the above-mentioned objectives, reducing the emission rate of vehicles stands in the first place. This is because of the existing tight governmental regulations concerning the environmental issues and global warming phenomenon, which have enforced industrialists to put a considerable amount of financial and technological forces on improving the performance of their products. In line with such a concern, environmental agencies and governmental authorities have exerted some provisions which oblige the automotive industry to move towards designing green vehicle technologies which emit a very trivial amount of pollutants [19]. Although the ultimate goal of the automotive industry is to replace the current gasoline-powered vehicles with electrified vehicles, this choice seems not to be feasible at the moment as there are still some technical problems for the widespread use of them. Furthermore, the initial investigations indicate that, by the current battery technologies, the production of fully electric vehicles is not an economical choice for both industrialists and consumers, and the final price as well as maintenance cost of electric drive vehicles is much more than that of gasoline-powered vehicles in the market. Therefore, control system designers and automotive engineers have been forced to focus on designing more effective controlling algorithms to decrease the emission rate of the current gasoline-powered vehicles [20].

1.2 Motivation

In general, reducing the amount of automobile emissions can be considered from different perspectives with regard to the type of pollutant and the stage of engine's operation. There is a fruitful literature dealing with analyzing the performance of automotive engines over a given driving cycle, and the interested readers can refer to seminal studies in this area by several active research groups [20-22]. By a precise analysis of the related research outcomes, one can understand that reducing the amount of hydrocarbon (*HC*) emissions is of the highest priority, because of the increasingly tight regulations concerned with this type of pollutants [23]. Various experiments have indicated that more than 80% of the total *HC* emissions for a typical driving cycle are generated during the first one or two minutes of the engine's working period, which is known as the coldstart period. This is mainly because the catalytic converter has not reached its nominal temperature, and also, its efficiency is far below the nominal value. Thus, for decreasing the amount of total tailpipe *HC* emissions of a given engine over a driving cycle, it is necessary to design high-performance controllers for reducing the *HC* emission rate over the coldstart period [24].

Through comprehensive experimental and theoretical studies with a given automotive engine by our colleagues in the Vehicle Dynamics and Control Lab at the University of California Berkeley, the following strategies have been suggested for developing effective controllers for reducing the *HC* emission rate during the coldstart period [25]:

(1) The first concept used by automotive engineers is to design coldstart controllers for reducing the required time for the warm-up procedure to assist the catalytic converter to reach its nominal efficiency in a very short period of time. This will result in a lower amount of the tailpipe *HCs* over the coldstart period.

(2) The second concept implies designing a controller for reducing the raw or engine-out *HC* emissions ($HC_{raw\text{-}c}$) over the coldstart period, which will consequently cause the reduction of cumulative tailpipe *HC* emission (HC_{cum}).

Due to the nonlinearity of engine's behavior over the coldstart period, designing an effective controller which can successfully satisfy the abovementioned concerns is a formidable task. Moreover, at the ideal case, a controller should be capable of handling both of the

abovementioned objectives, i.e. increasing the exhaust gas temperature (T_{exh}) and decreasing $HC_{raw\text{-}c}$, at the same time. However, coldstart experimental analyses have indicated that the abovementioned objectives are in confliction with each other, and thus, the controller should come up with an optimal trade-off between these two goals. On the other hand, the controller should be fast enough to process the states of the system and calculate the controlling commands in the very short period of time. Such concerns have gained a paramount attention among automotive control engineers and researchers and a vast number of controllers have been designed for the coldstart problem. Fortunately, the remarkable improvement of computational facilities and microprocessors has enabled control engineers to design much more powerful controlling algorithms, in particular predictive control strategies, to further improve the performance of automotive engines over the coldstart period [26].

In line with the recent interest towards designing more advanced controlling algorithms for the coldstart problem, in this thesis, different variants of model predictive controllers, i.e. nonlinear model predictive controller (NMPC), preference-based model predictive controller (PBNMPC), and receding horizon sliding controller (RHSC), are developed and evaluated for a given automotive engine. NMPC is a standard predictive controller which has successfully been applied to a wide range of control problems. PBNMPC is a novel predictive controlling strategy based on the Tchebycheff multi-objective programming which is best suited for coping with control problems dealing with a number of objective functions which are in confliction with each other. RHSC is another modified version of NMPC which incorporates the sliding model controller into the algorithmic structure of NMPC to optimally track a set of desired trajectories in a real-time fashion.

1.3 Outline

This thesis is organized into 5 chapters. In Chapter 2, a review of the most significant researches pertaining to the development of coldstart controllers is carried out. Chapter 3 is devoted to the detailed description of the mathematical structure of a control-oriented model used at the heart of the proposed coldstart controllers. Moreover, the results of a validation test carried out using the signals measured during a coldstart experiment are provided to ascertain the veracity of the control-oriented model. The descriptions of the adopted predictive controlling strategies together with the results of simulations for each controller are given in Chapter 4. Finally, the conclusions and potentials for future researches are presented in Chapter 5.

Chapter 2

Literature Review

In this chapter, a review of the existing coldstart control schemes and identification systems is carried out, and the findings and clues given by other active researchers are presented to further clarify the contribution of the current study. The investigations on the coldstart problem have been primarily followed in two different streams. A group of researchers have focused on the development of surrogate models to analyze the behavior of automotive engines over the coldstart period whilst another group of researchers have focused on the development of controllers for the coldstart operation. Here, the most important studies on the coldstart modeling and controller design together with their outcomes are reported to assist the readers learn the background of the existing literature.

By taking a precise look into the existing literature, one can easily realize that over the past decades, several researches have been carried out to modify the existing identification/controlling algorithms or proposing new strategies to reduce the amount of HC_{cum} emission during the coldstart period. Henein et al. [27] developed a model for analyzing cycle-by-cycle *HC* emissions during the coldstart operation of a gasoline engine. Based on the results, they concluded that the main reason to undesirable *HC* emissions is that the catalytic convertor is not warmed up over the coldstart period. Initially, the engine-out hydrocarbon emissions $HC_{raw\text{-}c}$ and the tailpipe emissions HC_{cum} are approximately the same, but once the catalytic convertor reaches the light-off temperature, it begins converting the combustion by-products, specifically unburned engine-out hydrocarbon emissions or HC_{raw}, at a better rate with a conversion efficiency of about 50%. Therefore, an attempt should be made to come up with effective and practical strategies to reduce the time required for catalytic convertors to reach the light-off temperature. It was also observed that T_{exh} has a remarkable contribution to providing the required heat for catalyst light-off. Hence, along with modeling of HC_{raw}, researchers have conducted a wide range of studies to analyze/model T_{exh} during the coldstart, as the other significant factor affecting the cumulative tailpipe *HC* emissions or HC_{cum}.

Dobner [28] utilized both linear and nonlinear modeling formulations to provide a dynamic model for controlling the main characteristics of a given engine. In that work, the author mainly focused on

modeling the throttle and the intake manifold dynamics of the engine. The results of this pioneering investigation have revealed that even an accurate linear regression model can be of great use for designing precise surrogate models for analyzing the complicated behavior of automotive engines over the coldstart period. The results of this investigation also demonstrated that the proposed models can be neatly utilized at the heart of real-time control algorithms to observe the real states of the engine and send proper commands to reduce the amount of HC_{cum}. Such interesting findings regarding the efficacy of linear and nonlinear regression models for the coldstart controller design has played a pivotal role in the progress of coldstart control research.

Later on, Moskwa and Hedrick [29] extended the results of Dobner's investigation and developed a compact model which was fast enough to be implemented inside real-time nonlinear coldstart controlling algorithms implemented based on the concept of sliding mode control and variable structures. One of the main advantages of the proposed model-based real-time controller was its capability to be used in conjunction with the controlling algorithms of other subsystems to come up with much more promising results. By validating the results of the controller using an instrumented engine, the authors demonstrated that their proposed surrogate model enjoys an acceptable generalization capability and can be used for different types of automotive engines.

Shaw and Hedrick [23] developed a simplified combustion model of automotive engines based on a heat release analysis which calculated the changes of hydrocarbon emissions (*HC*) as a function of the variations of air-fuel ratio (AFR) and idle speed. A nonlinear controller based on the sliding mode control technique was also developed to track the desired profiles of idle speed and AFR such that the catalytic converter reaches the warm-up temperature in a short period of time and the resulting *HC* emission is reduced as much as possible. The results of the conducted experiments clearly demonstrated that the proposed controller is capable of reducing HC_{cum} during the engine's coldstart period.

Zavala et al. [30] developed a state-space model to capture the fuel dynamics to improve the performance of coldstart hydrocarbon emission-reduction controllers of automotive engines. The model was then used within a model-based controller which offered the possibility of automating the controller design-to-implementation phase. During this analysis, for the first time, it was observed that acquiring a correct fuel-dynamics model can greatly improve the performance of coldstart controlling algorithms. Also, one of the main reasons of considering AFR in the coldstart model pertains to the fact that in spite of its importance for reducing HC_{cum} during the coldstart period, the

factory-supplied AFR sensor is not activated and no information regarding the AFR value is available in this condition. The results of the conducted experiments clearly demonstrated the efficacy of the developed controller for the coldstart problem.

Sanketi et al. [20] took advantage of a hybrid design approach to come up with a hybrid modeling/controlling method for reducing HC_{cum} over the coldstart period. The proposed hybrid model incorporated the related events during the coldstart period into their formulation. Also, the formulated hybrid controller was capable of switching between two alternative control modes. The first mode was designed with the primarily goal of reducing $HC_{raw\text{-}c}$ while the second module was developed to increase the temperature of catalytic converter as rapidly as possible to make sure that the catalytic converter works at the highest possible efficiency. Firstly, a reachability analysis was taken into account to theoretically verify the properties of the resulting closed-loop system. Thereafter, the controller was used for the coldstart control problem. Through an exhaustive comparative study, the authors demonstrated the efficacy of using a hybrid switching system for the coldstart control problem. Besides, the results of the comparative study indicated that the hybrid controller can surpass the standard nonlinear controllers, for instance sliding mode coldstart controllers.

In another study, Sanketi et al. [31] proposed an optimal controller via convex relaxations for reducing the amount of HC_{cum} during the coldstart period. Because of the simplicity of the implemented paradigm, the controlling commands could be calculated in a very short period of time. Moreover, the results indicated that the simple yet effective optimal controller resulting from convex relaxation mechanism is best suited for finding a trade-off between the two considered objective function terms of the controller. Given the nonlinearity of the coldstart control problem and the acceptable results obtained from this controller, it can be inferred that a proper convex relaxation methodology can be highly beneficial even for such nonlinear and transient processes. One of the advantages of the proposed controller pertains to its adaptive behavior which enables it to optimally make a trade-off between increasing T_{exh} and decreasing $HC_{raw\text{-}c}$ to come up with the most promising results.

Shen et al. [32] proposed a simple yet accurate mathematical model of a catalytic converter with 13-step kinetics and a 9-step oxygen storage mechanism which was capable of simulating the transient performance of the catalytic converter. The developed model considered the effect of heat transfer and catalyst chemical reactions as the exhaust gases flow through the catalyst. The

implemented heat transfer model consisted of the heat loss by the convection and conduction. Also, the model was capable of predicting the catalytic converter's performance over the coldstart period. Through experimental verifications, it was demonstrated that the results of the proposed model was in a good agreement with the experimental measurements, and the model could be used for model-based controller designs. In particular, the authors considered the US Federal Test Procedure (FTP) to study the catalytic converter's light-off characteristics. The simulation results demonstrated the potential of the proposed model to be used for real-world applications with different driving cycle patterns.

Chan and Hong [33] developed a heat transfer model to precisely analyze the chemical conversions of carbon monoxide and unburned hydrocarbons in the oxidation process during the coldstart period. The implemented model was then used to estimate the light-off time and the conversion efficiency of the catalyst. The implemented model also enabled analyzing the effects of water evaporation on the temporal distribution of exhaust gas temperature in the exhaust system. By exposing the developed model to experimentally measured signals, it was observed that the model has great potential to estimate the light-off time and conversion efficiency of automotive catalysts at different conditions based on the actual state of the system. This also showed the high authenticity of the heat transfer-based model for analysing the behavior of catalytic converters over the coldstart period.

Fiengo et al. [34] modified the existing models of catalysts and developed a control-oriented model to use at the heart of an optimal controlling technique for the warm-up phase of a three-way catalytic converter of a spark-ignition (SI) engine. To be more precise, the designed controller used the feedback of the temperature of the exhaust gas to calculate the optimum values of flow of air, the fuel into the cylinder, and the spark advance. The aim of the optimal controller was to minimize the total amounts of unburned hydrocarbons of the pre- and post-converter. Through an extensive comparative study, the authors demonstrated the efficacy of the proposed optimal controller in terms of the computational speed as well as its power to come up with the most optimum profiles. Furthermore, it was observed that considering the feedback of exhaust gas temperature can result in a stable and robust optimal controller which is suitable for real-time applications.

Zavala et al. [25] focused on the underlying physics of automotive engines and used wide spectra of experimental signals to simplify the structure of high-fidelity coldstart models and predict the controlling signals in a very short period of time to suite the resulting model for real-time applications. The model used a set of simple transfer functions together with the least square

estimation method to capture the dynamics of the system. One of the main advantages of the developed control-oriented model lied in its capability to predict the exhaust gas temperature, the catalytic converter's temperature, and the engine-out hydrocarbon emissions simultaneously, which enabled it to be used at the heart of real-time optimal multi-input multi-output (MIMO) controllers. Through a several sensitivity analysis, it was observed that considering the spark timing, AFR, and engine crankshaft speed as the controlling inputs for this coldstart model can afford the most optimal performance for predicting the considered engine's behaviour over the coldstart period. Based on the results of simulations, it was reported that the developed model can be used at the heart of real-time coldstart controllers to calculate the related controlling commands.

In most of the above-mentioned researches, the underlying physics of the engine was taken into account to come up with a model for calculating the most significant output variables during the coldstart period. In spite of the advantages of physics-based modeling, there is possibility that in some conditions, due to unknown disturbances and model uncertainties, a remarkable model/plant mismatch error occurs, which hinders the proper performance of devised model-based coldstart controller. This is mainly due to the fact that the behavior of engine is nonlinear and transient during the coldstart period, and it is very difficult to represent its performance accurately by means of a number of mathematical formulations. However, as mentioned before, it is highly important to come up with a sufficiently accurate surrogate model with less model/plant mismatches which can be used for representing the behavior of engine over the coldstart period with different initial operating and environmental conditions. One of the most important strategies which can be taken into account is the use of numerical and mesh-based modeling methodologies which enable automotive engineers to precisely investigate the characteristics of engines. This idea has come to the mind of researchers, and there exist some reports on the application of numerical modeling schemes for predicting the performance of automotive engines over the coldstart period.

For the first time, Jones et al. [35] took advantage of numerical modeling approaches to come up with a model based on fast response input/output measurements of the actual process. The developed model was capable of characterizing the significant dynamic behavior of engines under a variety of conditions. To ascertain the veracity of the developed model, a comprehensive experimental analysis under different environmental conditions and disturbances was carried out and the outcomes of the model were compared to those experimental signals. The results of the validation tests clearly indicated that the developed numerical model can accurately represent the actual behavior of the

considered engine and it enjoys from an acceptable accuracy. The promising results of this initial study instigated the authors of the paper to continue their investigations and seek for much more advanced numerical techniques to come up with more accurate surrogate models for automotive engine. In their second paper, some numerical methodologies were used to capture the dynamic behavior of a three-way catalyst converter over the coldstart period [36]. The model was then validated against a rich set of measured signals. After validating the model against the experimentally derived signals, it was used to analyze the performance of the catalytic converter to find out how its conversion efficiency can reach the nominal value in the shortest period of time. Also, the performed simulations indicated that the results of model can offer pragmatic solutions to expedite the warm-up period of the catalytic converter and changing its conversion efficiency to the nominal value in the shortest period of time.

Koltsakis and Tsinoglou [37] proposed a time-efficient 2-dimensional numerical modeling approach to analyze a close-coupled catalyst subjected to different exhaust gas conditions for automotive engines over the coldstart period. The numerical model considered the coupling between the problems of flow distribution and the conversion efficiency. The inputs to the model were obtained through a parametric study to find out the importance of various design parameters affecting the coldstart performance of close-coupled catalyst. Through extensive simulations, it was shown that the presented model enables studying the effect of catalyst insulation, and also, it was observed that the flow mal-distribution is not expected to affect the light-off during typical warming-up conditions.

Soumelidis et al. [38] proposed a numerical modelling scheme comprising of a library of four nonlinear dynamic models to estimate three-way catalyst transient responses. Each of the considered nonlinear models was optimized under certain operating regions such that the whole resulting model could accurately represent the behavior of the catalytic converter through all possible operating regions. The authors' claim was that the developed numerical model only requires the knowledge of upstream/downstream AFR and also can form the basis of an on-board catalyst monitoring and control system. The results of their simulations also indicated that the developed model can yield practical results and it has a high degree of accuracy.

Gonatas and Stobart [39] presented a black-box model for a given three-way catalytic converter for the real-time prediction of emission characteristics for both on-board control and diagnostics. The black-box model consisted of two components with similar structures. One was for the pre-catalyst

AFR prediction and one for the post-catalyst to estimate the individual gas concentration. In this study, the model was also used for the estimation of oxygen storage over the coldstart period. The authenticity of the proposed method was validated experimentally by means of hardware-in-the-loop simulations. The obtained results indicated that the method can be acceptable for real-time applications with a good level of accuracy. Also, the conducted experiments revealed that the use of black-box control-oriented models is a good approach for controlling the behavior of automotive engines over the coldstart period.

McNicol et al. [40] developed an automated expert-knowledge based decision-making methodology to come up with a satisfactory trade-off between the amounts of thermal energy delivered to the catalyst and the cumulative exhaust emission produced during the time before catalyst light-offs. The results of the conducted experiments revealed that the use of expert knowledge calibration methodology can result in a proper model suited for analyzing the performance of engines over the coldstart period. Besides, it was stated that one of the other main advantages of utilizing expert knowledge lies in the potential of the model to be expanded using additional information acquired from the engine by an expert engineer. Furthermore, the results of the conducted experiments unveiled that the proposed method can effectively withstand against the undesired effects of disturbances and uncertainties, which makes it a robust tool for analyzing the performance of the engine over a wide range of operating conditions.

Azad et al. [41] developed a black-box control-oriented model which was used at the heart of a sliding mode controller with bounded inputs for reducing automotive engine coldstart *HC* emissions. It was theoretically demonstrated that the devised model can be used at the heart of the coldstart controller to calculate the controlling commands within admissible operating bounds. The results of the simulations ascertain the veracity of the outcomes of the theoretical analysis for real-world applications, in particular the automotive coldstart problem. Besides, the results of simulations indicated that the devised sliding mode controller can neatly track desired profiles with an acceptable accuracy while satisfying the operating constraints. Azad et al. [8] extended their investigations and used a previously proposed control-oriented model to develop an optimal controller based on the Pontryagin's minimum principle (PMP) to control the behavior of an automotive engine over the coldstart period. The results of the simulations elaborated the veracity of the proposed controller for the coldstart problem. In particular, the results of the simulations showed that PMP is able to calculate the optimal controlling commands offline using the considered control-oriented model to

reduce HC_{cum} over the coldstart period such that the controlling commands always lay within certain ranges.

Salehi et al. [14] developed a hybrid switching controller to regulate the performance of an engine in a real-time fashion. The hybrid controller used a control-oriented model which was validated using different sets of experimental data. The controller comprised two independent modules working in cooperation with each other. One module was designed to expedite the catalytic warm-up procedure, and the other controlling module was developed to decrease the amount of $HC_{raw\text{-}c}$. It was experimentally demonstrated that an appropriate hyper-level supervisor can manage the interactions between the two modules to result in the most optimum performance of the considered engine.

Amini et al. [42] proposed a novel singular perturbation technique for the model-based control of automotive engine coldstart. For the control module, a sliding mode controller was taken into account. The singular perturbation was implemented based on the balanced realization principle, and the accuracy of the resulting model was proved experimentally. It was observed that the singular perturbation technique can be used to find out how to set the priority among different control actuators which have conflicting impacts on the desired control targets. The results also indicated that the proposed controller can show acceptable results for the coldstart control problem compared to other variants of model-based controllers.

Up to now, the most significant results of developing physics-based and numerical control, identification, and diagnostic tools for the coldstart problem have been reviewed. Besides, in one of the above-mentioned investigations, it was stressed that the use of expert knowledge for calibrating coldstart engine models can afford acceptable results. Additionally, it was stated that using a knowledge-based model can be advantageous to deal with the existing uncertainties and external disturbances. Such considerations have also come to the minds of other active research groups working on the engine coldstart control problem. The third stream of the conducted researches is devoted to the proposition of knowledge-based intelligent black-boxes for modeling the behavior of engines over the coldstart period to come up with powerful controlling algorithms. In what follows in this chapter, a review of the conducted research on the application of computational intelligence (CI) for modeling, monitoring, and controlling of automotive engine behaviors over the coldstart period is presented.

For the first time, the most significant contribution on using CI methods for the coldstart problem was made by Botsaris et al. [43]. In particular, a feed-forward artificial neural network (ANN) was used as an on-board diagnosis system to predict the catalyst performance over the coldstart period. To train ANN, different set of databases were gathered using two specific kinds of catalysts in a laboratory bench at idle speeds. The simulation results indicated that ANN could neatly represent the behavior of engine over the coldstart period, and thus, it was claimed that it can be used for model-based system analyses and online controller designs. In spite of the promising reports of the mentioned research, the application of CI for the coldstart problem remained barren until recently where different types of soft computing techniques were used for developing coldstart models.

Mozaffari and Azad [44] developed an optimally pruned extreme learning machine (OP-ELM) with ensemble of regularization techniques and negative correlation penalty for the high-fidelity modeling of a given engine's behavior over the coldstart period. The developed model was compared to a set of models existing in the literature, and it was reported that OP-ELM has high potentials for representing the complex behavior of engine over the coldstart period. The proposed model was also capable of estimating multiple outputs at the same time which enabled it to be used for evaluating MIMO coldstart controllers. Furthermore, it was observed that CI methods with regularization techniques allow signal processing capabilities, which is beneficial for removing redundant information from given datasets, and thus, results in a much more compact model.

In another study [45], Mozaffari and Azad extended the results of their first investigation and proposed an ensemble neuro-fuzzy radial basis network with self-adaptive swarm-based supervisor and negative correlation for the compact modeling of engine's behaviour during the coldstart period. The outcomes of the simulations clearly indicated that the fuzzy rules obtained from neural learning could accurately represent the engine's transient and nonlinear behavior over the coldstart period. Besides, in their numerical simulations, the performance of the devised model was validated using a wide range of experimental data. Also, the robustness of the model was examined using different uncertain datasets, and it was observed that, the fuzzy rules can effectively suppress the undesired effects of uncertainties.

Following the investigations on CI-based coldstart models, Mozaffari and Azad [46] adopted a well-known CI-based modeling tool, known as Gaussian generalized regression neural network, which was optimized using an evolutionary algorithm to analyze the performance of catalytic converters over the coldstart period. The results of the conducted simulations indicated that the

adopted CI-based model was capable of estimating the performance of considered engine system under different conditions. Besides, it was observed that the developed CI-based model has a higher robustness compared to some well-known physics-based models available in the literature. All in all, the archived literature clearly demonstrates the importance of analyzing the behavior of automotive engines over the coldstart period to reduce the amount of HC_{cum}.

In spite of the extensive reports in the literature on modeling and control of automotive coldstart operations, there are several open questions which still need much more consideration, and are worth further investigations. In particular, as it can be inferred from the literature, the potential of model-based predictive control strategies has not been investigated thoroughly for the coldstart problem. Given the fact that a lot of effort has been exerted on developing control-oriented models for the engine coldstart phenomenon, in this thesis, our focus will be on designing model-based controllers rather than developing new control-oriented coldstart models. Therefore, as described in the next chapter, an authentic control-oriented model for the coldstart operation of a given engine is adopted from the literature, and it is used for designing and evaluating the performance of different types of predictive coldstart controllers in the rest of the thesis. After presenting the related simulation results, finally, some conclusions are reported which further enrich the existing literature, and can be of great use for automotive researchers working on the coldstart control problem.

Chapter 3

Control-oriented Model for Coldstart Operations

This chapter is organized into two subsections. Firstly, the experimental setup required for activation of the plant, namely a Toyota Camry engine, is presented. Thereafter, the mathematical formulation of a coldstart control-oriented model proposed by our research group colleagues at the University of California, Berkeley (UCB) is discussed.

3.1 Experimental Setup

As the engine over the coldstart period has a nonlinear dynamic behaviour and various decision parameters and elements play a role in its performance, it is a challenge to develop a physics-based model for the system, and thus, it is easier to use a black-box model and tune it through the experimental signals coming from standard design of experiment (DoE) tests. Following such a philosophy for developing a control-oriented model requires an experimental setup which enables capturing a set of empirical signals. To create the experimental setup, an instrumented Toyota Camry internal combustion engine (ICE) equipped with a number of sensors is taken into account. The experimental bed belongs to the Vehicle Dynamics and Control Lab (VDL) at UCB. The instrumented ICE engine is shown in Fig. 3-1. The test equipment used for measuring the experimental signals is also depicted in Fig. 3-2

The engine has four cylinders with multi-port fuel injectors, along with an intake air control valve. It has also the capability of producing up to 117 KW power at 5600 rpm. To simulate the engine loads, the engine is coupled to a dynamometer. A dyno-controller is used to regulate the speed and torque of the dynamometer. To measure the important signals of the considered ICE, for instance air/fuel ratio (AFR), a number of sensors are taken into account. Also, an emission analyzer is utilized for measuring the rate of HC emissions. The abovementioned setup is used to capture the required information for developing a control-oriented model. In the next subsection, the formulation of the control-oriented model is presented.

Figure 3-1 UCB's coldstart experimental bed

Figure 3-2 Test equipment: a) dynamometer, b) external Panel and c) FID hydrocarbon analyzer

3.2 Control-oriented Model

Through an experimental sensitivity analysis, it was observed that there are a limited number of variables which remarkably affect the variations of T_{exh} and $HC_{raw\text{-}c}$ for the considered ICE over the coldstart period. These quantities are the spark timing (Δ), AFR, and engine's speed (ϖ_e). The sensitivity analysis and simple regression tests also indicated that there is a first order linear-like relation, but with offsets and saturations, between the variations of the input signals, i.e. $u_1 = \Delta$ (deg. ATDC) + 50, u_2 = AFR, and $u_3 = \varpi_e$, and the corresponding changes in T_{exh} and $HC_{raw\text{-}c}$. Such observations brought our colleagues at UCB to the conclusion that a number of ordinary differential equations (ODEs) can be coupled altogether for creating a control-oriented model for representing

the engine's coldstart behaviour. The formulated ODE representation of the coldstart state-space model is given below [8]:

$$
\begin{aligned}
\dot{x}_1 &= \frac{u_1}{\tau_1} + -\frac{k_1}{\tau_1} x_1 \\
\dot{x}_2 &= \frac{u_3}{\tau_2} + \frac{k_2}{\tau_2} x_2 \\
\dot{x}_3 &= \frac{16 - u_2}{\tau_3} + \frac{k_3}{\tau_3} x_3 \\
\dot{x}_4 &= \frac{u_3 - 800}{\tau_4} + \frac{k_4}{\tau_4} x_4 \\
\dot{x}_5 &= \frac{16 - u_2}{\tau_5} + \frac{k_5}{\tau_5} x_5 \\
\dot{x}_6 &= \frac{|u_1 - 55| + (u_1 - 55)}{2\tau_6} + \frac{k_6}{\tau_6} x_6
\end{aligned}
\tag{3-1}
$$

The values of the internal parameters of the above control-oriented model are listed in Table 3-1. It is worth mentioning that the second and fourth states are only functions of the engine speed which is a known signal, and thus, are not considered for the implementation of the predictive controllers.

Table 3-1 Internal parameter values for the control-oriented model

τ_1	τ_2	τ_3	τ_4	τ_5	τ_6
2.9629	156.2661	0.1800	1.1667	0.0002	0.0150
k_1	k_2	k_3	k_4	k_5	k_6
0.1997	5.2708	0.8527	0.1667	0.001	0.0075

From the above 6 state equations, the first three are used to find the values of T_{exh}, and the last three state equations are used to determine the values of $HC_{raw\text{-}c}$. The standard formulation used for the estimation of those output signals are, as follows:

$$T_{exh}(t) = \max\left(x_1(t) + x_3(t), 0\right) + x_2(t) \tag{3-2}$$

$$HC_{raw-c}(t) = \max\left(4000 - x_4(t), 800\right) + \max\left(x_5(t) + x_6(t), 0\right) \tag{3-3}$$

where, T_{exh} and $HC_{raw\text{-}c}$ are in $^{\circ}C$ and *ppm*, respectively.

To prepare the developed model to be used at the heart of predictive controllers, it is mandatory to reformulate the above differential state-space model in a difference state-space form. Using the Runge-Kutta method, the discrete-time form of the state-space model given in Eq. (3-1) can be given, as follows:

$$
\begin{aligned}
x_1(k) &= \delta t \cdot \frac{u_1(k-1)}{\tau_1} + \left(1 - \frac{\delta t \cdot k_1}{\tau_1}\right) x_1(k-1) \\
x_2(k) &= \delta t \cdot \frac{u_3(k-1)}{\tau_2} + \left(1 - \frac{\delta t \cdot k_2}{\tau_2}\right) x_2(k-1) \\
x_3(k) &= \delta t \cdot \frac{16 - u_2(k-1)}{\tau_3} + \left(1 - \frac{\delta t \cdot k_3}{\tau_3}\right) x_3(k-1) \\
x_4(k) &= \delta t \cdot \frac{u_3(k-1) - 800}{\tau_4} + \left(1 - \frac{\delta t \cdot k_4}{\tau_4}\right) x_4(k-1) \\
x_5(k) &= \delta t \cdot \frac{16 - u_2(k-1)}{\tau_5} + \left(1 - \frac{\delta t \cdot k_5}{\tau_5}\right) x_5(k-1) \\
x_6(k) &= \delta t \cdot \frac{\left|u_1(k-1) - 55\right| + \left(u_1(k-1) - 55\right)}{2\tau_6} + \left(1 - \frac{\delta t \cdot k_6}{\tau_6}\right) x_6(k-1)
\end{aligned}
\tag{3-4}
$$

To make sure that the control-oriented model works properly, a validation test for certain input signals has been carried out. Figure 3-3 compares the experimental data versus the control-oriented model predictions for T_{exh} and $HC_{raw\text{-}c}$. It is clear that the model has a good correlation with the experimental data, which makes it a good fit to the coldstart control design.

The input signals should be confined within a logical range. To do so, the physical behavior of the engine should be taken into account. One way to reduce the coldstart *HC* emissions is to increase T_{exh} as fast as possible to warm-up the catalytic converter, and thus, enhance its conversion efficiency. Traditionally, this has been accomplished by the spark timing retard strategy. However, retarding the spark timing can lead to reduced engine torques, which will cause a potential drivability issue. Furthermore, exposing the catalytic converter to excessive T_{exh} can generate more thermal stresses and reduce its service life. Therefore, the spark timing retard should have a limit.

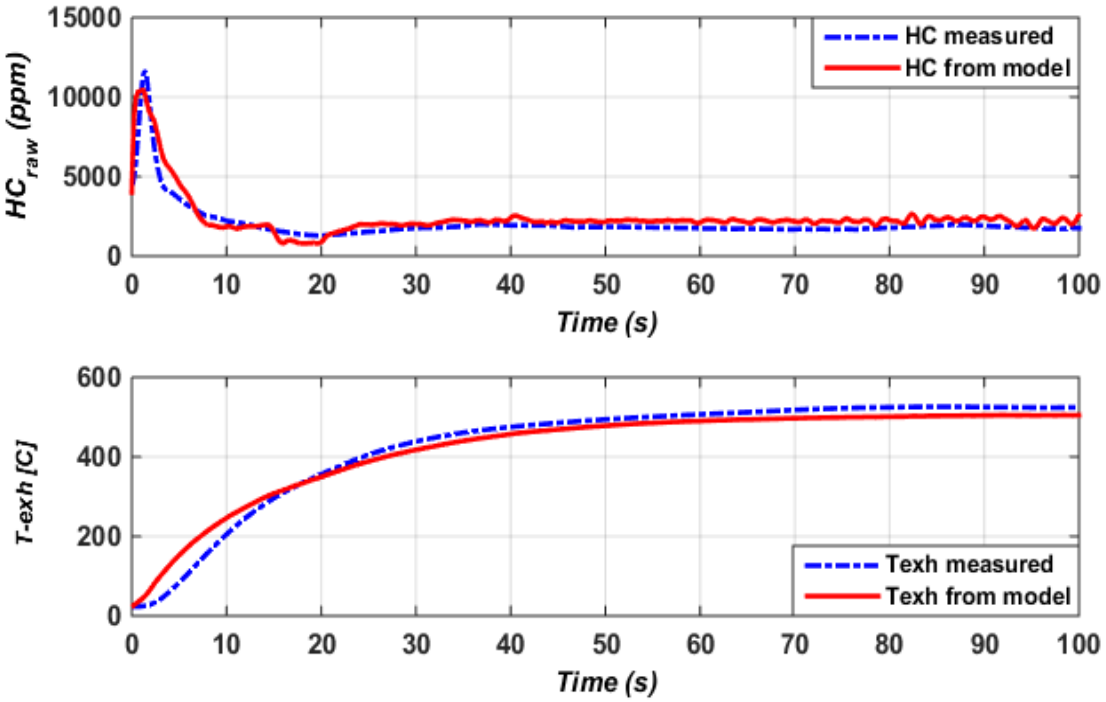

Figure 3-3 Validation of the model against experimental signals

Another method to reduce the coldstart *HC* emissions is to use a lean fuel strategy, which is equivalent to a higher *AFR*. However, this may cause the combustion instability. Thus, to avoid this problem, there should be a higher value for *AFR*, as well.

Based on the above-mentioned practical considerations, the first two inputs are confined within the ranges below:

$$\begin{aligned} 40^{\circ} \le u_1 \le 60^{\circ} \\ 10 \le u_2 \le 16 \end{aligned} \tag{3-5}$$

The input signal u_3 is considered as a known external input. Given this fact, the engine system states can be represented as $\mathbf{x} = [x_1, x_3, x_5, x_6]$ because, at every time step, the other variables x_2 and x_4 can be calculated beforehand using the values of signal u_3.

As mentioned previously, the value of HC_{cum} depends on the conversion efficiency of catalyst (η). Based on experimental observations [19], the following equation has been proposed for η:

$$\eta = (1-\eta_1)(1-\eta_2) \tag{3-6}$$

where:

$$\eta_1(k) = \exp\left(-a_1\left(\frac{\max\left(u_2(k),0\right)-\lambda_0}{\Delta\lambda}\right)^{m_1}\right) \tag{3-7}$$

$$\eta_2(k) = \exp\left(-a_2\left(\frac{\max\left(T_{cat}(k),T_{cat0}\right)-T_{cat0}}{\Delta T_{cat}}\right)^{m_2}\right) \tag{3-8}$$

The equation parameters, that is, a_1, a_2, m_1, and m_2, have been identified by experimental data. The catalyst temperature (T_{cat}) primarily depends on T_{exh} as the exhaust gas temperature is a major source of the catalyst warm-up. These quantities are approximately proportional:

$$T_{cat}(k) = k_{cat} \cdot T_{exh}(k) \tag{3-9}$$

Finally, the following equation can be used to determine the value of HC_{cum}:

$$HC_{cum} = \int_0^T (1-\eta)\dot{HC}_{raw} \cdot dt = \int_0^T (1-\eta)\dot{m}_{exh}\left(\frac{16}{28.5}\times 10^{-6}\right) HC_{raw-c} \cdot dt \tag{3-10}$$

Based on experimental observations, the exhaust mass flow rate $\dot{m}_{exh}$ is approximately proportional to u_3:

$$\dot{m}_{exh} = b_1 u_3 + b_2 \tag{3-11}$$

The considered control-oriented model can be used at the heart of any discrete-time model-based controller to calculate the coldstart controlling signals. Having said that the formulated objective function for each predictive controlling strategy is specific. Thus, based on the above-mentioned model, different types of objective functions are defined to design different versions of predictive optimal controlling strategies for the coldstart problem in the next chapter.

Chapter 4

Coldstart Predictive Control Strategies

This chapter is devoted to the detailed descriptions of the proposed predictive control strategies, namely nonlinear model predictive controller (NMPC), preference-based model predictive controller (PBNMPC), and receding horizon sliding controller (RHSC), as well as presenting their results for controlling the considered engine over the coldstart period. At the end of this chapter, some important remarks can be inferred regarding the applicability of predictive control strategies for the coldstart control problem.

4.1 Nonlinear Model Predictive Controller (NMPC)

The first considered controller is a standard model-based predictive optimal controller which is suited for nonlinear controlling problems. The controller consists of two important parts. The first part is the controlling module which works based on predicting the future behavior of plant. The second part of NMPC is an optimization module which is suited for optimizing nonlinear objective functions. The detailed formulation of the proposed controller is presented in the rest of this subsection, and finally, the results of simulations together with a number of comparative numerical tests are given to assess the potentials of the standard NMPC to deal with the coldstart problem.

4.1.1 Controller Formulation

Recently, nonlinear model predictive controllers have gained a remarkable attention from control engineers due to their efficient performances [46, 47]. Such controllers are, in particular, effective for a process in which a good model representing the plant behavior is available. The potential of NMPC controllers for making decisions based on the prediction of future behavior of the system enables them further enhance the quality of control commands, as compared to the other control techniques [48]. A comprehensive literature review together with detailed descriptions of different NMPC formulations can be found in [49]. For the sake of brevity, here, we avoid providing the details and background information of NMPC design technique as it has extensively been done before. Rather,

the focus of this subsection will be on developing the mathematical formulation of NMPC controller for the coldstart problem.

Let us consider the following state-space representation of the system:

$$\chi(k+1) = \mathbf{f}\left(\chi(k), \upsilon(k), \phi_{\chi}, k\right) \tag{4-1}$$

where ϕ_{χ} shows the parameters of the model **f**, and χ and υ are the augmented state and input matrices, as follows:

$$\chi(k) = \begin{bmatrix} x_1(k) \\ x_1(k) \\ \vdots \\ x_6(k) \end{bmatrix}; \qquad \upsilon(k) = \begin{bmatrix} u_1(k) \\ u_2(k) \\ u_3(k) \end{bmatrix} \tag{4-2}$$

Two sequential signals are captured after every δt *sec*, which is calculated by $\delta t = \frac{H_P}{N}$. As it can be inferred, the time-difference depends on the prediction horizon and the number of set points. The initial values of the states are also set as given below:

$$\chi_0 = \begin{bmatrix} \frac{T_{cat0}}{3k_{cat}} = 11.25 & 11.25 & 11.25 & 0 & 0 & 0 \end{bmatrix}^T \tag{4-3}$$

Let us now assume that T_{exh} and $HC_{raw\text{-}c}$ are derived using the following equations:

$$T_{exh}(k) = \mathbf{q}\left(x_1(k), x_2(k), x_3(k), \phi_{T_{exh}}, k\right) \tag{4-4}$$

$$HC_{raw-c}(k) = \mathbf{h}\left(x_4(k), x_5(k), x_6(k), \phi_{HC_{raw-c}}, k\right) \tag{4-5}$$

The output vector of the plant, *y*, can be derived found by:

$$y(k) = \begin{bmatrix} T_{exh}(k) \\ HC_{raw-c}(k) \end{bmatrix} \tag{4-6}$$

As mentioned previously, the input signals u_1 and u_2 are confined within a predefined range. However, there are more constraints concerned with the variations of inputs (Δu) over the control

horizon (H_u) that should be considered. Here, these additional constraints are taken into account to eliminate the input signal oscillations, as given below:

$$\begin{cases} \Delta\hat{u}_1(k+i\,|\,k) - 0.02\left(u_1^{\max} - u_1^{\min}\right) \le \Delta\hat{u}_1(k+i+1\,|\,k) \le \Delta\hat{u}_1(k+i\,|\,k) + 0.02\left(u_1^{\max} - u_1^{\min}\right) \\ \Delta\hat{u}_2(k+i\,|\,k) - 0.02\left(u_2^{\max} - u_2^{\min}\right) \le \Delta\hat{u}_2(k+i+1\,|\,k) \le \Delta\hat{u}_2(k+i\,|\,k) + 0.02\left(u_2^{\max} - u_2^{\min}\right) \end{cases} \quad (4\text{-}7)$$

The augmented matrix derived from the equation above can be expressed by:

$$\Delta\upsilon(k) = \begin{bmatrix} \Delta u_1(k) \\ \Delta u_2(k) \end{bmatrix} \quad (4\text{-}8)$$

The above-mentioned equations represent the states, outputs and inputs of the system only for one set point. However, to proceed with the NMPC calculations, we need to define more general matrices to include the present and future predicted values. Such an implementation is necessary for the calculations of the NMPC controller's objective function for pre-defined control and prediction horizons. If the control and prediction horizons at each working point are indicated by H_P and H_u, respectively, these general matrices can be defined as:

$$U = \begin{bmatrix} \hat{\upsilon}(k\,|\,k) \\ \hat{\upsilon}(k+1\,|\,k) \\ \vdots \\ \hat{\upsilon}(k+H_u-1\,|\,k) \end{bmatrix}; \qquad \Delta U = \begin{bmatrix} \Delta\hat{\upsilon}(k\,|\,k) \\ \Delta\hat{\upsilon}(k+1\,|\,k) \\ \vdots \\ \Delta\hat{\upsilon}(k+H_u-1\,|\,k) \end{bmatrix} \quad (4\text{-}9)$$

$$X = \begin{bmatrix} \chi(k+1\,|\,k) \\ \chi(k+2\,|\,k) \\ \vdots \\ \chi(k+H_P\,|\,k) \end{bmatrix}; \qquad Y = \begin{bmatrix} y(k+1\,|\,k) \\ y(k+2\,|\,k) \\ \vdots \\ y(k+H_P\,|\,k) \end{bmatrix} \quad (4\text{-}10)$$

The objective function at the heart of NMPC can be given as follows:

$$J(k) = \sum_{i=1}^{H_P} \left(1 - \hat{\eta}(k+i\,|\,k)\right) \dot{m}_{exh}(k+i\,|\,k) \left(\frac{16}{28.5} \times 10^{-6}\right) \hat{HC}_{raw-c}(k+i\,|\,k) + \sum_{i=0}^{H_u-1} \left\|\Delta\hat{u}_1(k+i\,|\,k)\right\| + \left\|\Delta\hat{u}_2(k+i\,|\,k)\right\| \quad (4\text{-}11)$$

where, H_P represents the prediction horizon, H_u indicates the control horizon, and $(k + i \mid k)$ shows the prediction at time step $k + i$ based on its value at time step k. The second term of the objective function was added to the original formulation for HC_{cum} to make sure that the control input signals

determined over the control horizon will be smooth and do not show illogical oscillations. The above objective function, i.e. *J (k)*, can be easily solved at each working point *k*.

By solving the objective function, the optimum profiles of the input signals, namely $\boldsymbol{v}^*$, for the upcoming horizon can be determined. The obtained profile is used by the controller to reduce the value of HC_{cum}. In most of the cases, the updating time of the controller t_u is less than the time required for the completion of H_P. Let us investigate this concept mathematically:

$$\begin{cases} N \in \mathbb{Z} \,/\, H_P = N \cdot \delta t \\ m \in \mathbb{Z} \,/\; t_u = m \cdot \delta t \end{cases} \quad \& \quad m < N \tag{4-12}$$

The above equation indicates that the optimizer used for the NMPC controller should be fast enough to complete the calculations in a time period shorter than t_u to guarantee the proper performance of the controller. Obviously, the best control performance can be achieved if one can reduce the updating time (t_u) and increase the prediction horizon (that is, the value of *N*) as much as possible, at the same time.

Figure 4-1 indicates a schematic illustration of the NMPC control operation for HC_{cum} reduction as well as the notion of prediction horizon, updating time, and control horizon.

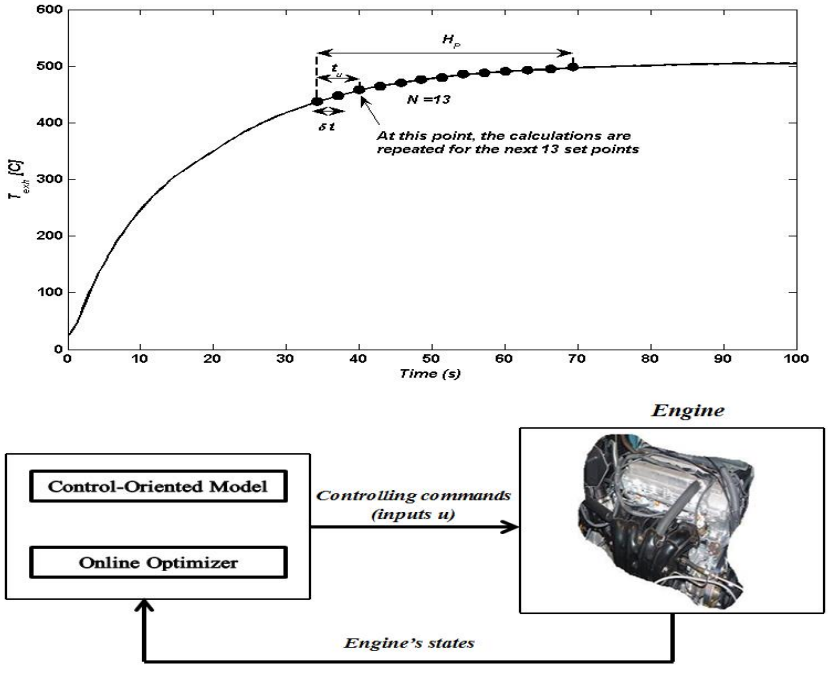

Figure 4-1 Schematic illustration of NMPC

4.1.2 Online Optimizer

In the previous subsections, we indicated that for the NMPC controller implementation, the considered optimizer should be powerful enough to converge to the optimum solution, and also, fast enough to terminate the required calculations in a very short period of time. Recently, multi-agent bio-inspired optimizers have successfully been applied for NMPC control applications and demonstrated their capability for meeting the above-mentioned criteria [50, 51]. In the light of such promising reports, here, we have been motivated to test the potential of an advanced bio-inspired population-based optimizer (DPSO) for the coldstart control problem. In this subsection, a detailed description of DPSO is provided.

DPSO combines the notions of social interactions among species with microbial life in the nature [52]. Numerical investigations have demonstrated that DPSO is a good fit for optimization problems in which the objective landscape dynamically varies over time. The initial algorithmic structure of DPSO includes several random parameters and random samplings. This can increase the exploration capability of DPSO for complex landscapes. However, as an online optimizer at the heart of NMPC controller, some revisions should be exerted to its structure to make sure that a certain degree of exploitation among its agents is guaranteed, which in turn results in the convergence of the algorithm. To this aim, here, we modify the structure of DPSO slightly to boost the exploitation rate among its agents. It is necessary to mention that the revisions are only exerted on the control parameters of algorithm and the structure of DPSO remains unchanged. The main reason behind increasing the exploitation (convergence speed) of DPSO lies in the fact that the online optimizer for the NMPC controller should be capable of finding an acceptable optimum profile in a very short period of time (less than t_u) [49].

The original DPSO technique, known as dynamic hybrid PSO (DHPSO), has four main operators, namely, the detection of dynamic changes, updating particles positions, reproduction and aging [52]. Based on our assessment, the last two operators can be removed from the structure of DHPSO as they increase the computational complexity and foster the exploration of agents. As an NMPC solver, DPSO which includes some mechanisms for the dynamic change detection and position updating, can show a very fast convergence to an acceptable solution. Also, its algorithmic structure enables us performing a mathematical analysis to make sure that the convergence can be guaranteed. The important feature of DPSO/DHPSO is the ability of detecting the dynamical change. Therefore, this

phase remains unchanged. Let us consider each agent of DPSO as a particle. The algorithmic structure of DPSO is given below:

Initialization: DPSO has three main parameters, namely $N_{p,min}$, $N_{p,max}$ and N_{sentry}, which should be specified beforehand. Firstly, $N_{p,max}$ particles are initialized randomly. Then, the initialized particles are divided into two sub-populations. In this way, the first $N_{p,min}$ particles are sent to the first sub-population and the remaining particles are sent to the second sub-population. The velocity of each particle (V) is randomly generated as well.

Detection of dynamic changes: At the beginning of optimization, at each updating point of the control procedure, a detection mechanism is carried out to find out whether the control objective function experiences any change. In this context, a pre-defined number of sentry particles, N_{sentry}, are distributed over the solution space randomly. At the beginning of each optimization stage, their fitness values are evaluated. If the fitness value of at least one of these sentry particles changes, it can be inferred that the objective function undergoes a dynamic change. This means that DPSO should re-organize its exploration/exploitation capabilities to be reconciled to the new solution landscape. Once a dynamic change is detected, the fitness of all $N_{p,max}$ particles are re-evaluated and the best $N_{p,min}$ particles are put into the first sub-population. The remaining particles are re-initialized, and then, sent to the second sub-population. This strategy is very efficient for dynamic environments. On the one hand, the experiences from the previous exploration/exploitation over the solution space are preserved. On the other hand, the re-initialized particles give DPSO a flexibility to search with a wider vision over the solution landscape, and possibly, identify the fruitful regions within the solution space.

It is worth pointing of that the sentry particles do not participate in the optimization and are just used for detecting possible dynamic changes in the solution space. Hence, the convergence of DPSO depends on the behavior of the other particles.

Updating particles position: To update the position of all particles, the local best position of particles (*lbest*) and the global best solution are found by DPSO, *gbest*, and the average position of the solutions in the second sub-population (*ave*) should be determined. For a D dimensional problem, the position of particle i at iteration t can be defined as $Z_i^t = \left[z_i(t,1), z_i(t,2), ..., z_i(t,D) \right]$.

Let us show $lbest_i$, *gbest*, *ave*, and the velocity vector as:

$$lbest_i^t = [l_i(t,1), l_i(t,2), ..., l_i(t,N)] \quad (4\text{-}13)$$

$$gbest^t = [g(t,1), g(t,2), ..., g(t,N)] \quad (4\text{-}14)$$

$$abest^t = \left[a(t,1), \mathrm{a}(t,2), ..., \mathrm{a}(t,D)\right] \quad (4\text{-}15)$$

$$V_i\ (t) = \left[v_i(t,1), v_i(t,2), ..., v_i(t,D)\right] \quad (4\text{-}16)$$

Then, the updating rule of the particles can be implemented as below:

$$V_i^{t+1} = \omega^t V_i^t + \psi\left(gbest - Z_i^t\right) + \kappa\left(ave - Z_i^t\right) + \mu\left(lbest_i - Z_i^t\right) \quad (4\text{-}17)$$

$$Z_i^{t+1} = Z_i^t + V_i^{t+1} \quad (4\text{-}18)$$

where ω, ψ, and μ are the inertia weight, social coefficient, and cognitive coefficient, respectively. κ is a new parameter which verifies the impact of the re-initialized solutions in the second sub-population on the searching characteristics of DPSO. As it can be inferred, the mentioned parameters play a pivotal role on the movement of agents through the solution space.

Termination: After a pre-defined number of iterations (*t*), the optimization procedure is terminated and the optimal profiles are used to control the coldstart operation of ICE.

The algorithmic structure of DPSO is presented in Figure 4-2.

4.1.3 Parameter Settings and Simulation Setup

There are a few parameters which should be set prior to proceeding with the simulations. The multi-agent optimizer for the NMPC calculations possesses some controlling parameters which should be verified. For ω spanning [0,0.7298] and $\psi + \mu + \kappa$ within the range of [0, 1.7], it can be assured that, eventually, DPSO converges to a stable point. At each stage of the calculations, DPSO terminates the procedure once the difference between the objective values of two sequential iterations becomes very small. DPSO performs the optimization with 20 particles from which the first half are sent to the first sub-population and the remaining particles are sent to the second sub-population. To ascertain the veracity of DPSO, two well-known optimization methods, golden search (GS) and sequential quadratic programing (SQP) are taken into account.

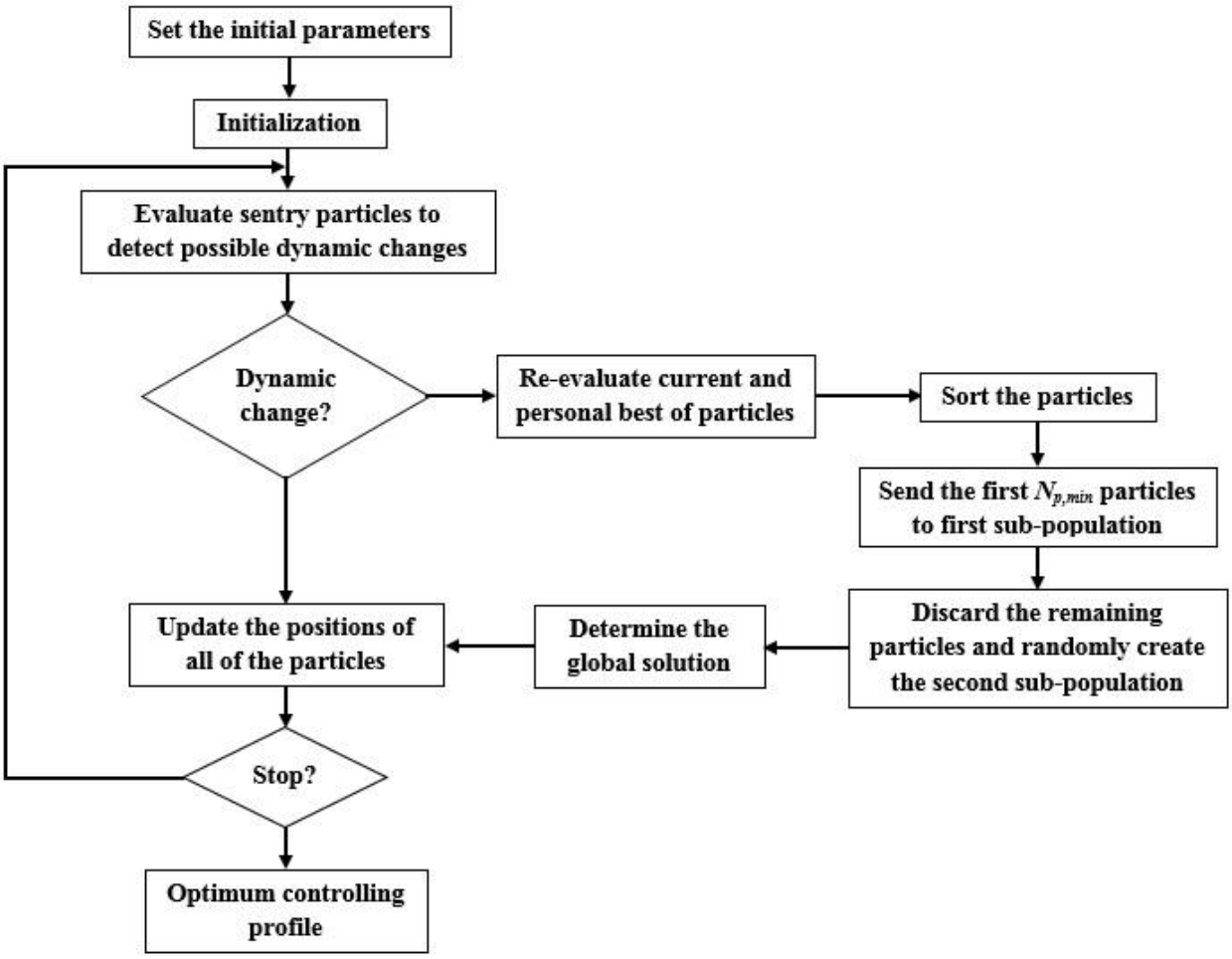

Figure 4-2 Flowchart of the DPSO technique

For the GS algorithm, which is a sequential mini-max searching mechanism, the steps presented in [53] are taken into account. If a change in the values of objective function between two sequential iterations becomes very small, GS terminates its operation. SQP is also implemented based on the steps described in [49]. The rival optimization techniques are implemented using Matlab. For SQP, the existing Matlab solver is used, and the GS algorithm is encoded in a Matlab M-file. The stopping criterion of GS is the number of iteration number and equals to 30, and the stopping criterion of SQP is the convergence which is at the heart of Matlab's SQP optimization tool.

For the classical optimal controller, the PMP algorithm is considered. The detailed descriptions of the steps required for the implementation of PMP can be found in [8].

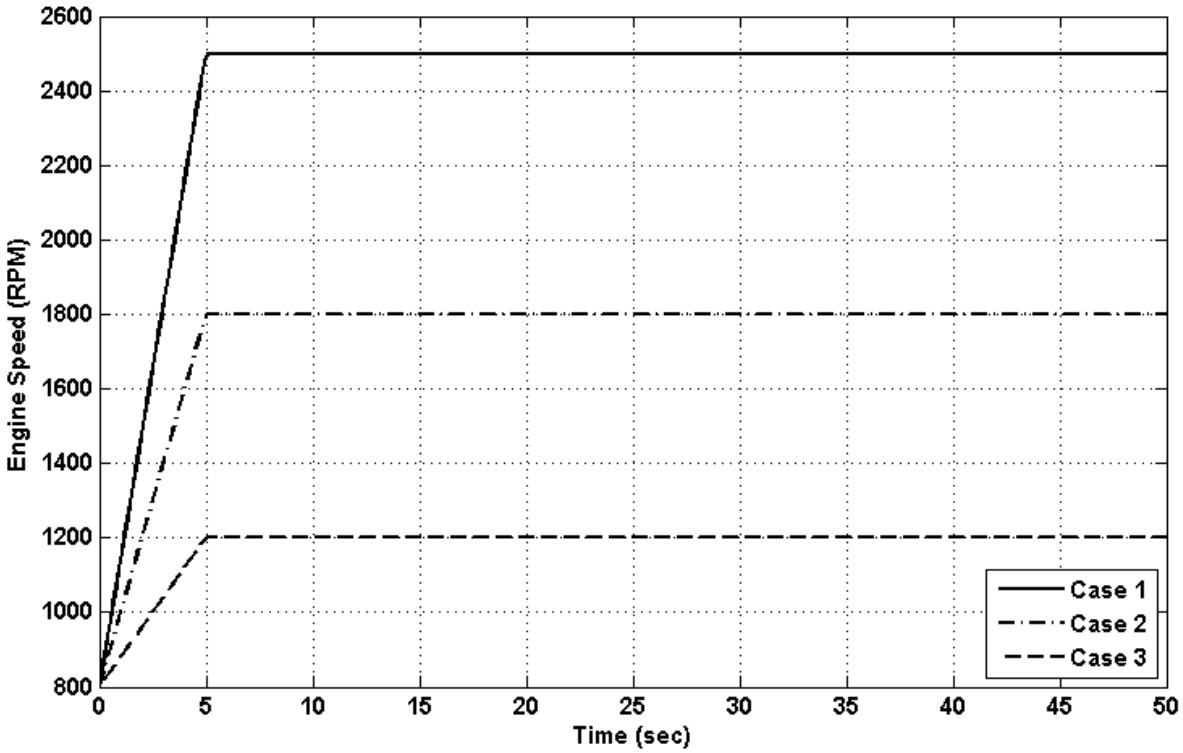

Figure 4-3 Considered engine speed profiles during the coldstart period (external inputs)

The engine speed profile ($u_3 = \varpi_e$) is treated as a known external input and should be fed to the devised NMPC controller during the coldstart period. For all of the simulations in this thesis, we conduct the simulations for three different engine speed profiles, to check the performance of the control system for different coldstart scenarios. The considered engine speed curves are depicted in Figure 4-3.

All of the simulations are carried out using the Matlab software with Microsoft Windows 7 operating system on a PC with a Pentium IV, Intel core i7 CPU and 4 GBs RAM.

4.1.4 Simulation Results

In this subsection, two important objectives are pursued. Firstly, it is tried to conduct a comparative study to investigate different features of the NMPC controller. This stage of the simulations includes

the evaluation of the efficacy of DPSO for the considered control problem, the robustness of DPSO, and the performance of the NMPC controller compared to the rival classical optimal controller designed based on PMP. At the second stage of simulations, the impact of prediction horizon (H_P) on the performance of the controller is investigated.

Based on a comparative study as well as our own assessment, for the first stage of the simulations, the prediction horizon of 2 *sec* and the number of updating points of 15 are considered. The NMPC controller re-calculates the input signals after every 0.26 *sec*. Table 4-1 lists the total HC_{cum} resulting from the NMPC computations with the DPSO, SQP and GS online optimizers as well as the required time for the calculation of control commands at each stage of the process. It is worth noting that the reported calculation time is the average of all calculations that an optimizer performs over the entire control process. In this way, we will make sure that the reported time is a proper indicator of the computational efficiency of each method. For all of the three cases, it can be seen that the computational complexity of DPSO and GS are relatively the same and the both are more time-consuming than SQP. Also, the results indicate that DPSO can yield better optimum solution compared to GS and SQP. The other interesting observation relates to the better performance of SQP in comparison with GS although it has less calculation time. This, in turn, implies that SQP is a better online optimizer compared to heuristic methods; however, it cannot outperform DPSO. This is mainly due to the efficient exploration/exploitation capability of the agents of DPSO. Given the fact that the differences between the calculation time of SQP and DPSO never exceeds 0.04 *sec*, it can be inferred that DPSO is a suitable online optimizer to be used at the heart of NMPC controller. As mentioned before, DPSO is a multi-agent optimizer which uses stochastic operators, in the form of random walks, to search the solution domain. This means that the solution suggested by DPSO may not be the same over independent runs. If the variations of the obtained results over independent runs become too large, the performance of NMPC controller can be degraded significantly. Therefore, a numerical experiment is carried out to check the robustness of DPSO. Obviously, the higher robustness of DPSO provides the better control performance. For checking the robustness of DPSO, there is no choice but to repeat the optimization for a number of independent runs and calculate the variation of the obtained solutions in terms of the standard variation (*std.*). Here, the optimization procedure is repeated for 10 independent runs for each of the three cases. Table 4-2 presents the details of the obtained results in terms of the calculation time and total HC_{cum}. Also, the statistical results representing the main aspects of the NMPC computations for independent runs are reported in Table 4-3.

Table 4-1 Comparison between the NMPC control performances with different online optimizers

Algorithms	*Case 1*		*Case 2*		*Case 3*	
	Calculation time	HC_{cum}	*Calculation time*	HC_{cum}	*Calculation time*	HC_{cum}
SQP	0.039679	0.2321	0.038322	0.2335	0.036345	0.2353
GS	0.049294	0.2443	0.053316	0.2485	0.065345	0.2495
DPSO	0.060549	0.2105	0.061424	0.2187	0.073467	0.2251

Table 4-2 Performance of the NMPC controller over 10 independent runs

# Run	*Case 1*		*Case 2*		*Case 3*	
	Calculation time	HC_{cum}	*Calculation time*	HC_{cum}	*Calculation time*	HC_{cum}
1	0.060549	0.2105	0.061424	0.2187	0.073467	0.2251
2	0.061322	0.2104	0.061812	0.2165	0.076564	0.2256
3	0.060835	0.2079	0.061333	0.2280	0.072929	0.2274
4	0.061500	0.2207	0.061463	0.2144	0.077763	0.2173
5	0.061337	0.2094	0.062092	0.2187	0.070773	0.2172
6	0.060856	0.2152	0.064675	0.2131	0.076469	0.2102
7	0.061416	0.2156	0.061416	0.2265	0.072382	0.2296
8	0.060329	0.2094	0.061337	0.2224	0.074392	0.2126
9	0.061416	0.2199	0.061322	0.2168	0.077670	0.2358
10	0.062150	0.2203	0.061506	0.2147	0.075762	0.2190

Table 4-3 Statistical results of the NMPC computations for independent runs

# Run	*Case 1*		*Case 2*		*Case 3*	
	Calculation time	HC_{cum}	*Calculation time*	HC_{cum}	*Calculation time*	HC_{cum}
Best	0.0608	0.2079	0.0646	0.2131	0.0729	0.2102
Worst	0.0614	0.2207	0.0613	0.2280	0.0777	0.2358
Mean	0.0612	0.2139	0.0618	0.2190	0.0748	0.2220
Std.	5.3e-4	0.0050	0.0010	0.0051	0.0024	0.0080

By taking a peek at the obtained results, it can be seen that the NMPC calculation results over the independent runs are very close to each other. This issue can be even further verified by considering the low *std*. values. As it can be seen, the differences of the best, worst, and mean values of the total emitted HC_{cum} are negligible. The results augur the high robustness of the utilized online optimizer at the heart of NMPC controller. This further endorses on the applicability of DPSO for NMPC control applications.

After ensuring the acceptable performance of the controller with online DPSO optimizer, we intend to compare its performance with an optimal control strategy designed based on PMP. This is basically an offline controller which uses the same control-oriented model (but in its differential equation form) to determine the optimal input profiles. PMP can afford the global optimum profiles; however, that is difficult to implement it as an online control algorithm because the calculation of the

optimal solution over the coldstart period takes a few minutes. In the previous work by our research group, it has been mentioned that the use of steepest descent method for PMP will slow down the optimization process, and thus, hinders its applicability for online control applications [8]. However, to deal with the plant model uncertainties and unknown disturbances, it is necessary to implement real-time controllers for automotive coldstart applications. The proposed NMPC controller uses fresh information about the engine system and performs an online optimization based on this information (see Figure 4-1). However, when the pre-defined optimum inputs calculated offline by the PMP algorithm are applied to the real engine, the control performance may be degraded significantly, due to mismatches between the control-oriented model and the engine system. It is now important to find out how much the near-optimal, but real-time, solutions suggested by the NMPC calculations are different from those obtained by PMP. To be more precise, it is critical to make sure that the online optimization performed by the NMPC controller does not reduce the quality of the optimum profiles.

Table 4-4 compares the results obtained by the PMP and NMPC control techniques. As it can be seen, the difference between the mean performance of online NMPC and that of offline PMP controls are not significant. This means that the NMPC technique can be reliably used to develop a real-time controller for reducing HC_{cum} over the coldstart period.

Prior to starting the second stage of numerical experiments, we would like to investigate the physical behavior of the engine system by providing the obtained profiles.

Figure 4-4 indicates the optimum *AFR* profiles obtained by the NMPC controller. It can be inferred that, to minimize HC_{cum}, the proportion of air/fuel mixture should always remain lean ($AFR \approx 15$-16). Figure 4-5 depicts the optimum profiles of spark timing. As it can be seen, for all of the three cases, the NMPC controller leads the value of Δ from 5 deg. BTDC to 10 deg. ATDC within the first 10 seconds and retains the profile at the relatively same degree for the remaining 40 seconds. As it was indicated in Table 4-4, when the engine speed is at the highest level, the minimum of HC_{cum} is the lowest. This is mainly due to the fact that by increasing the engine speed, the debit of $\dot{m}_{exh}$ is increased. Figure 4-6 depicts the profile of T_{exh} for the three cases. It can be seen that by increasing the engine speed, the exhaust gas temperature increases. This means that more heat is provided to increase the catalyst temperature which in turn incurs a faster catalyst warm-up. According to Figure 4-7, such a behavior results in an increase in the value of catalyst conversion efficiency. Figure 4-8 indicates the real-time raw *HC* emission rate. For all of the three cases, there is a peak in the engine-out *HC* emission rate. The experiments have shown that this initial peak is necessary for reducing the

risk of engine stalling. It can be also inferred that by increasing the engine speed, the rate of engine-out *HC* emissions reduces to lower levels in a shorter period of time.

Table 4-4 Results obtained by the online NMPC and offline PMP controllers

Controller	*Case 1*	*Case 2*	*Case 3*
PMP	0.145	0.158	0.218
NMPC	0.213	0.219	0.222

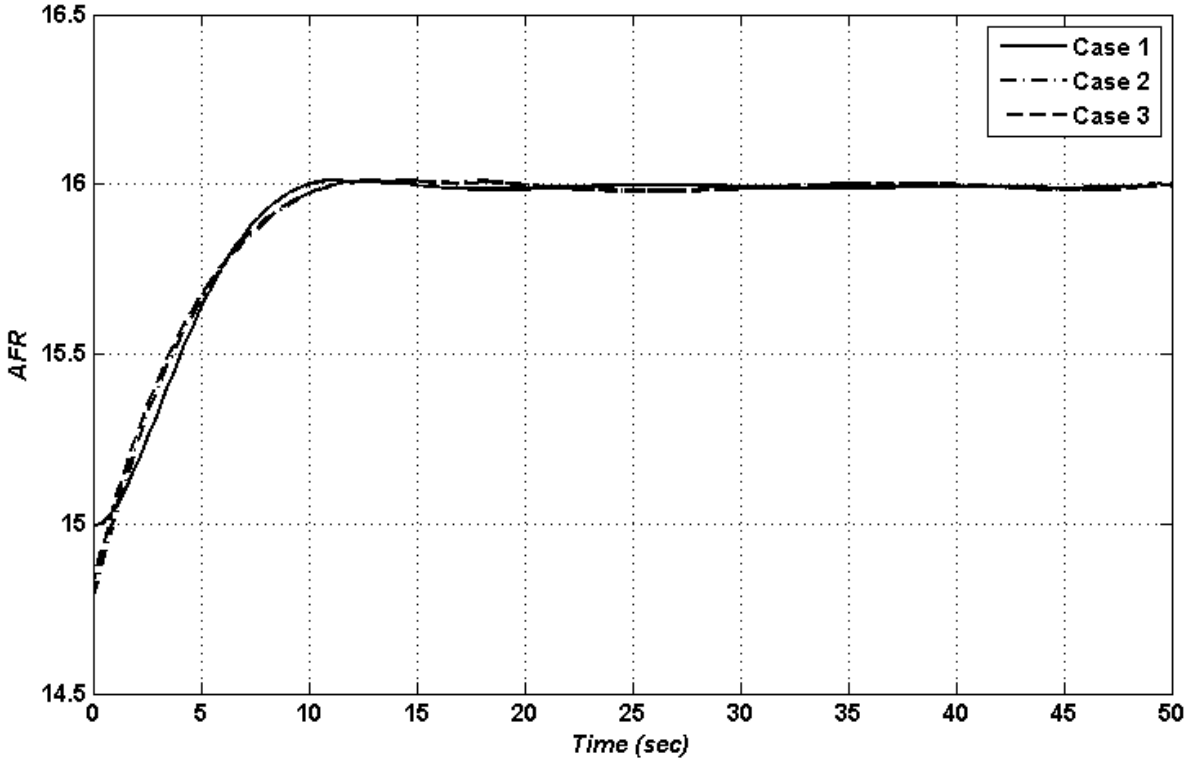

Figure 4-4 Optimum AFR profiles obtained by NMPC

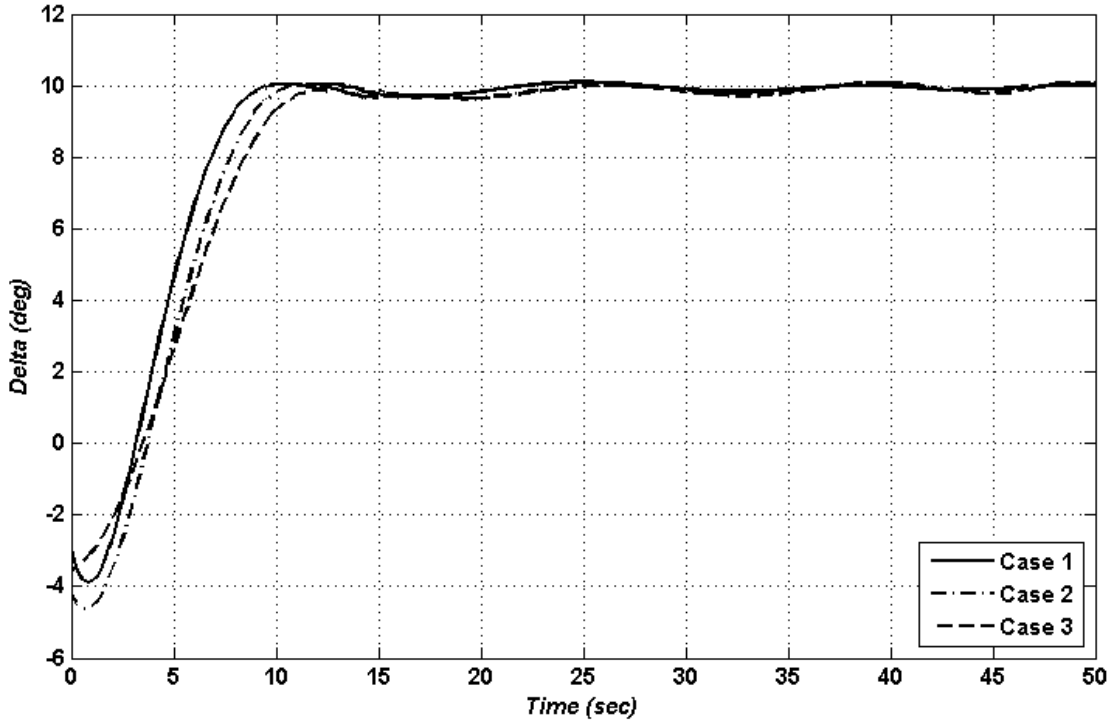

Figure 4-5 Optimum Δ profiles obtained by NMPC

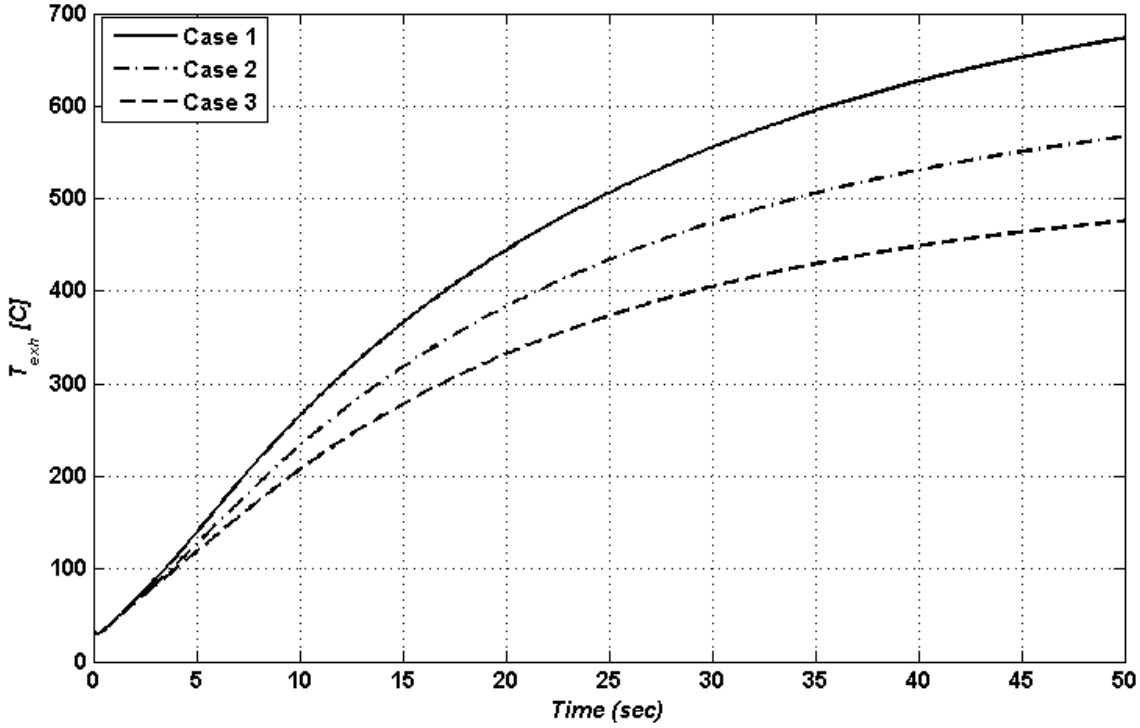

Figure 4-6 Optimum T_{exh} profiles obtained by NMPC

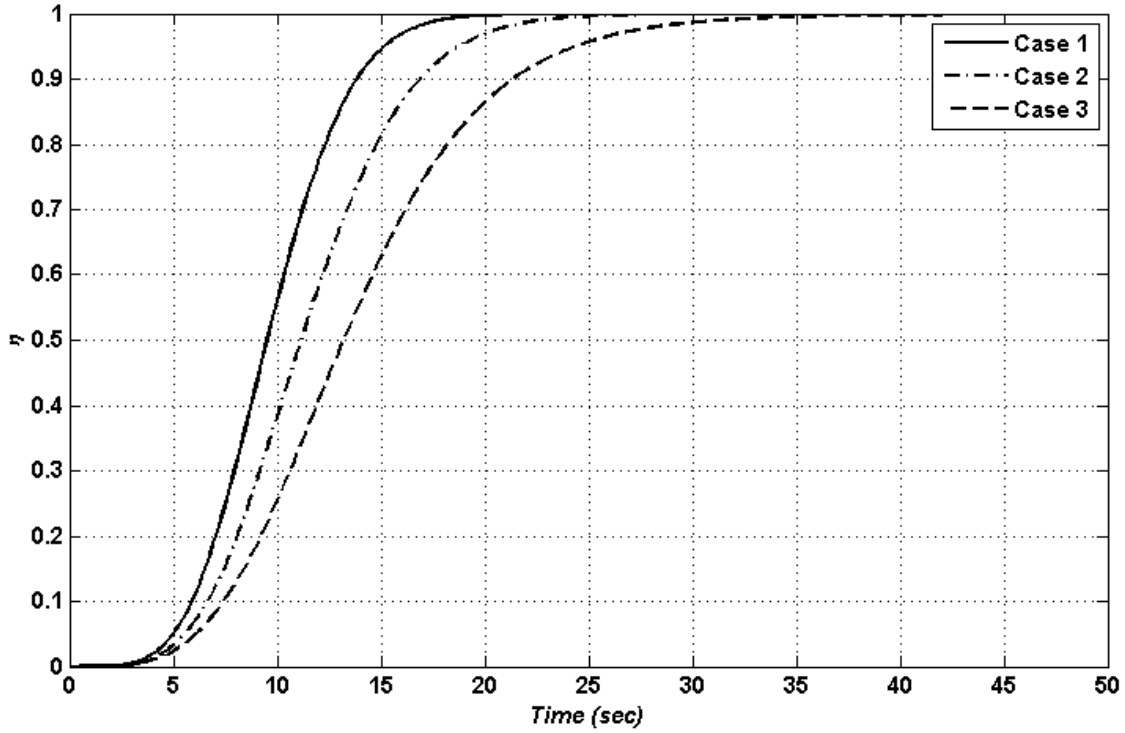

Figure 4-7 Catalyst efficiency for the optimum solutions

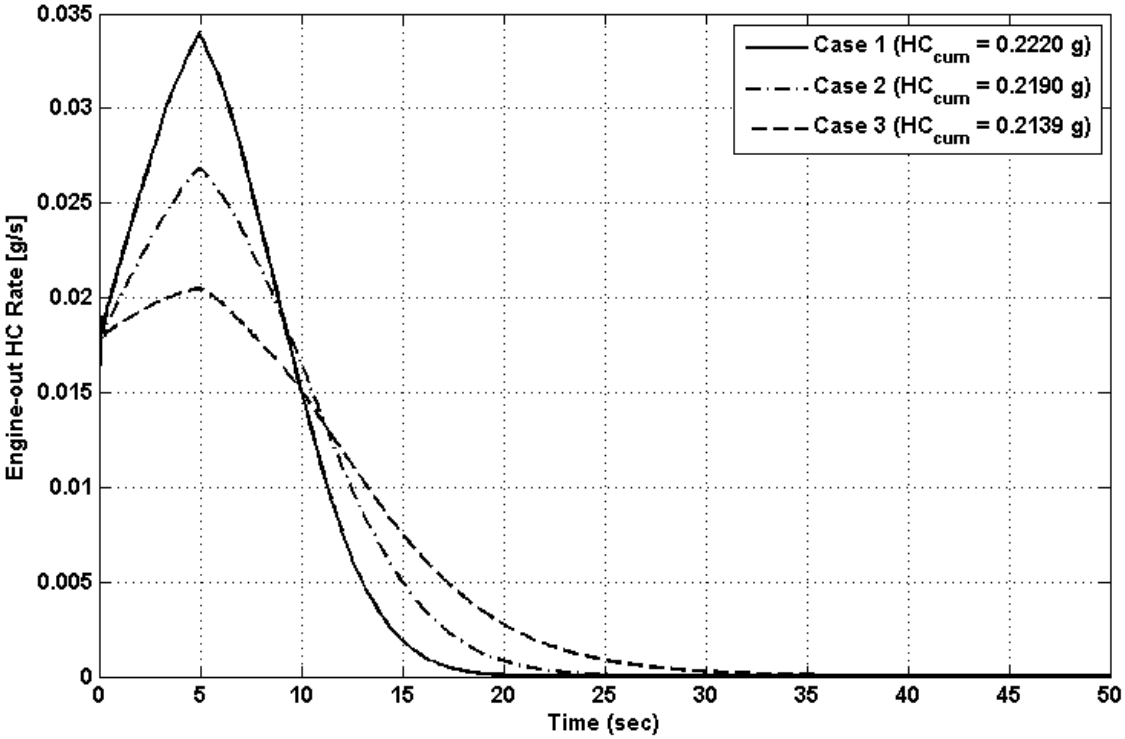

Figure 4-8 Engine-out *HC* emissions rate for the optimum solutions

In the second stage of the numerical experiments, the impact of prediction horizon length on the performance of controller is evaluated. For this sake, the control action calculation procedure is repeated for 6 different prediction horizons, that is, 1, 2, 3, 4, 5, and 6 *sec*. It is worth pointing out that the number of set points for each stage of the calculations is adjusted so that the values of updating time (t_u) and δt remain constant. Table 4-5 presents the results of the simulations. As it can be seen, by increasing the length of H_P, the value of HC_{cum} is reduced. However, this results in an increase in the calculation time. It is interesting that for H_P of 6 *sec*, the total emitted *HC* is relatively the same as that for PMP. However, as it can be seen, the calculation time exceeds the updating time, and thus, the results are not suitable for practical applications. Therefore, for implementing the proposed NMPC coldstart controller in real-time, we have no choice but to accept the near-optimal solutions at the expense of lower computational costs.

The results of simulations indicated that the NMPC technique can outperform the PMP algorithm in terms of the computational efficiency for the coldstart problem. Also, through a theoretical analysis, it was demonstrated that the proposed multi-agent optimization DPSO technique can guarantee the convergence of the NMPC calculations within a finite number of iterations. Moreover, the comparative results indicated that the proposed multi-agent optimizer can outperform golden search (GS) and sequential quadratic programming (SQP) for calculating the control commands. The numerical experiments also indicated that by increasing the prediction horizon as well as the number of updating points, the results of the NMPC calculations can be improved. However, it was observed that to achieve such better results in terms of the performance optimality, a higher computational budget is required, and thus, there is a trade-off between the optimality and online implementation potential of the NMPC controller.

Table 4-5 Performance of the NMPC controller with different prediction horizons

H_P *(sec)*	*Case 1*		*Case 2*		*Case 3*	
	Calculation time	HC_{cum}	*Calculation time*	HC_{cum}	*Calculation time*	HC_{cum}
1	0.0586	0.2185	0.0579	0.2205	0.0674	0.2313
2	0.0612	0.2139	0.0618	0.2190	0.0748	0.2220
3	0.0675	0.1847	0.0683	0.1912	0.0894	0.2214
4	0.0854	0.1845	0.0912	0.1886	0.0988	0.2205
5	0.1442	0.1772	0.1231	0.1824	0.1425	0.2201
6	0.1546	0.1453	0.1423	0.1653	0.1562	0.2186

4.2 Preference-based Nonlinear Model Predictive Controller (PBNMPC)

In this section, we scrutinize the mathematical steps required for the development of PBNMPC controller. This section is given into 4 subsections. In the first subsection, the system constraints are formulated, and also, an approach is presented which tightens the constraints dynamically to ensure the control commands do not show illogical changes over the coldstart period. In the second subsection, the standard formulation of NMPC for the coldstart problem is given, and also, it is explained how we can use the system states to define a receding horizon for the sake of predictive control. The next subsection describes how the concept of Tchebycheff analysis can be employed to develop an objective function based on the control engineer's preferences. Moreover, the detailed steps for defining the desired profiles, as well as their dynamical adaption are presented. Finally, in the last subsection, it is expressed how MQFSA can be used to solve the non-smooth objective function derived from the Tchebycheff analysis.

4.2.1 System Input Constraints

To make sure that the PBNMPC controller sends feasible commands to the engine system, it is necessary to confine the input signals within a logical range. To determine the ranges for the inputs, there is no choice, but to investigate the underlying physics of ICE system. As discussed before, in this context, the control commands should always fall within the following ranges:

$$\begin{cases} 40^{\circ} \le u_1 \le 60^{\circ} \\ \\ 10 \le u_2 \le 16 \end{cases} \tag{4-19}$$

Again, the input signal u_3 is assumed to be given, which means that at each working point, the values of x_2 and x_4 can be calculated, and thus, the engine system states will be only: $\mathbf{x} = [x_1, x_3, x_5, x_6]$.

The formulation of PBNMPC approach enables us add more constraints to the control problem to increase the feasibility and practicality of the control commands. To be more to the point, here, we limit the rate of the input signals variations over the prediction horizon. This means that for a certain value of the control command at time step k, the possible value of input signal for the next time step $(k + 1)$ falls within a specific range. This introduces a dynamic constraint over the control horizon,

which can be taken into account properly by MPC controllers. The mathematical formulations of these constraints are given below:

$$\begin{cases} \hat{u}_1(k+i-1|k)-\Delta\hat{u}_1(k+i|k)\le\hat{u}_1(k+i|k)\le\hat{u}_1(k+i-1|k)+\Delta\hat{u}_1(k+i|k) \\ \hat{u}_2(k+i-1|k)-\Delta\hat{u}_2(k+i|k)\le\hat{u}_2(k+i|k)\le\hat{u}_2(k+i-1|k)+\Delta\hat{u}_2(k+i|k) \end{cases} \tag{4-20}$$

where, $(k + i \mid k)$ shows the prediction at time step $k + i$ based on its value at time step k, and Δu represents the possible variation range of the input signal from a certain time step $k + i - 1$ to the next time step $k + i$. The possible variation range of the input signals is calculated by:

$$\begin{cases} \Delta\hat{u}_1(k+i-1|k)-0.02\left(u_1^{\max}-u_1^{\min}\right)\le\Delta\hat{u}_1(k+i|k)\le\Delta\hat{u}_1(k+i-1|k)+0.02\left(u_1^{\max}-u_1^{\min}\right) \\ \Delta\hat{u}_2(k+i-1|k)-0.02\left(u_2^{\max}-u_2^{\min}\right)\le\Delta\hat{u}_2(k+i|k)\le\Delta\hat{u}_2(k+i-1|k)+0.02\left(u_2^{\max}-u_2^{\min}\right) \end{cases} \tag{4-21}$$

4.2.2 Controller Formulation

By significant advancements of computational tools and processors, optimal predictive controllers have been attracting remarkable attention from control engineers. The applicability of such controllers has been started, first, by using them for controlling chemical processes. Later, such types of controllers have been successfully applied to much more intricate process control tasks. The research literature has clearly demonstrated the potential of optimal predictive controllers for the calculations of control commands based on a system's future behavior, which turns this type of controller into one of the most promising control systems, compared to the other types of controllers [47, 54]. In this subsection, the mathematical formulation of the considered control strategy is described, and also, it is explained how it can be used for HC_{cum} emission reduction during the coldstart period. It is worth mentioning that the formulation below establishes the most critical part of PBNMPC controller. The state-space representation of the engine system given in the previous chapter can be shown in the following nonlinear algebraic form:

$$\mathbf{X}(k+1)=\mathbf{f}\left(\mathbf{X}(k),\mathbf{U}(k),\phi_\chi,k\right) \tag{4-22}$$

where, ϕ_{χ} is the matrix of the internal parameters of the system, **f** represents a set of discrete nonlinear equations, and also, **X** and **U** are the augmented forms of the state and the input matrices, respectively, given below:

$$\mathbf{X}(k)=\begin{bmatrix} x_1(k) \\ x_1(k) \\ \vdots \\ x_6(k) \end{bmatrix}; \qquad \mathbf{U}(k)=\begin{bmatrix} u_1(k) \\ u_2(k) \\ u_3(k) \end{bmatrix} \tag{4-23}$$

Similar to the previous controller design, the initial values of the states are:

$$\mathbf{X}(0)=\begin{bmatrix} 11.25 & 11.25 & 11.25 & 0 & 0 & 0 \end{bmatrix}^{T} \tag{4-24}$$

As a discrete system, the time interval of the state-space representation should be verified. The NMPC controller uses two key parameters to calculate the control commands at each updating point. These parameters are the prediction horizon (H_P) and the number of set points (N) considered for discretizing H_P. Based on the above-mentioned concepts, the time interval δt is given by:

$$\delta t=\frac{H_P}{N} \tag{4-25}$$

It is worth noting that the values of the above parameters can be adjusted to make sure that the predictive controller works properly to achieve high-performances in real-time applications. At each set point, the engine system outputs T_{exh} and $HC_{raw\text{-}c}$ can be calculated, and thus, the augmented output matrix is given by:

$$\mathbf{Y}(k)=\begin{bmatrix} T_{exh}(k) \\ HC_{raw-c}(k) \end{bmatrix} \tag{4-26}$$

Another matrix which should be defined is the augmented form of the input signals variations:

$$\Delta\mathbf{U}(k)=\begin{bmatrix} \Delta u_1(k) \\ \Delta u_2(k) \end{bmatrix} \tag{4-27}$$

Now, the key point is the way of assembling the above parameters and information to construct the predictive controller for our case study. This can be done by applying the concept of receding

horizon as well as the creation of a proper objective function (**J**). Thus, the first step is to define more general matrices to concatenate the present and future values of the above augmented matrices. Let us consider that at each updating point of the controller calculations, the computations should be performed for a pre-defined control horizon (H_U) and prediction horizon (H_P).

The general form of the receding horizon-based matrices for **U** and $\Delta\mathbf{U}$ are given by:

$$\hat{\mathbf{U}}^* = \begin{bmatrix} \hat{\mathbf{U}}(k|k) \\ \hat{\mathbf{U}}(k+1|k) \\ \vdots \\ \hat{\mathbf{U}}(k+H_U-1|k) \end{bmatrix}; \qquad \Delta\hat{\mathbf{U}}^* = \begin{bmatrix} \Delta\hat{\mathbf{U}}(k|k) \\ \Delta\hat{\mathbf{U}}(k+1|k) \\ \vdots \\ \Delta\hat{\mathbf{U}}(k+H_U-1|k) \end{bmatrix} \tag{4-28}$$

Also, the general form of the receding horizon-based matrices for **X** and **Y** are expressed by:

$$\mathbf{X}^* = \begin{bmatrix} \mathbf{X}(k|k) \\ \hat{\mathbf{X}}(k+1|k) \\ \vdots \\ \hat{\mathbf{X}}(k+H_P|k) \end{bmatrix}; \qquad \mathbf{Y}^* = \begin{bmatrix} \mathbf{Y}(k|k) \\ \hat{\mathbf{Y}}(k+1|k) \\ \vdots \\ \hat{\mathbf{Y}}(k+H_P|k) \end{bmatrix} \tag{4-29}$$

Using the above information, a proper objective function **J** will be defined for the NMPC controller, as follows:

$$\mathbf{J} = \sum_{i=1}^{H_P} \left\| \hat{\mathbf{Y}}^*(k+i|k) - \mathbf{Y}_d(k+i|k) \right\|_{Q(i)}^2 + \sum_{i=0}^{H_u-1} \left\| \hat{\mathbf{U}}^*(k+i|k) \right\|_{\mathrm{R}(i)}^2 \tag{4-30}$$

By optimizing the above objective function, the optimum values of control commands $\mathbf{U}^*$ for the upcoming horizon will be determined. Obviously, the optimization algorithm should be fast enough to calculate the proper commands in a very short period of time.

In many of the existing optimal coldstart controllers, such as NMPC, equation below has been used as the objective function **J**:

$$\mathbf{J} = \sum_{i=1}^{H_P} \left\| \left(1-\hat{\eta}(k+i|k)\right) \dot{m}_{exh}(k+i|k) \left(\frac{16}{28.5} \times 10^{-6} \right) \hat{HC}_{raw-c}(k+i|k) \right\|_{Q(i)}^2 + \sum_{i=0}^{H_u-1} \left\| \hat{\mathbf{U}}^*(k+i|k) \right\|_{\mathrm{R}(i)}^2 \tag{4-31}$$

As it can be seen, the above objective function depends on several quantities, including the conversion efficiency which increases the complexity of computations. This is a critical issue when using the controlling technique in real-time as the required calculations should be done in a very short period of time. To overcome such an important problem, in the formulation of PBNMPC, a modified objective function with less complexity will be employed to calculate the control commands much faster. Moreover, instead of using sequential quadratic programming (SQP), a very fast and robust optimization algorithm will be applied which is best suited for solving the non-smooth, non-convex optimization problem within the PBNMPC formulation. Through simulations, it will be indicated that the proposed objective function is very efficient for the coldstart HC_{cum} reductions.

4.2.3 Tchebycheff preference for desired trade-offs

As mentioned previously, there is a dilemma on how to change the input signals during the coldstart to minimize HC_{cum} because there is a trade-off between the variations of T_{exh} and $HC_{raw\text{-}c}$ in response to the inputs [55]. From a mathematical perspective, the Pareto theory states that the confliction between two arbitrary quantities $\boldsymbol{f_1}$ and $\boldsymbol{f_2}$ can result in a non-dominated front known as the Pareto front. The optimal Pareto front refers to a curve which includes a number of solutions resulting from the optimal trade-offs between $\boldsymbol{f_1}$ and $\boldsymbol{f_2}$. To be more to the point, this theory expresses that in such a condition, it is impossible to come up with a unique optimum solution and there exist a lot of optimum pairs of $\boldsymbol{f_1}$ and $\boldsymbol{f_2}$ which can be considered as the optimized solution to a conflicting objective function **J**. Hence, formulating a simpler objective function for the coldstart problem purely based on T_{exh} and $HC_{raw\text{-}c}$ can lead the NMPC controller (or any other optimal controller) towards various input profiles. One remedy to this challenging confliction is to define weights for the both T_{exh} and $HC_{raw\text{-}c}$ to direct the control strategy towards certain profiles, as given below:

$$\mathbf{J} = \min : \lambda_1 f_1 + \lambda_2 f_2 \tag{4-32}$$

Considering two conflicting quantities with the above form helps the optimizers always seek for a particular trade-off. However, there is no guarantee that the final solution converges to the optimum Pareto front. To be more precise, for a certain trade-off, there is also a possibility that the quality of the final solution can be further improved. The Tchebycheff approach is a mean for converting the problem of approximating a Pareto front into a number of preference-based scalar optimization

problems such that the global optimality of the final solution is guaranteed. The Tchebycheff form of the above objective function is given by:

$$\mathbf{J} = \min : \max\left\{\lambda_1 \left| f_1 - z_1^* \right|,\ \lambda_2 \left| f_2 - z_2^* \right|\right\} \tag{4-33}$$

where, z shows the reference point and is calculated, as follows:

$$\begin{cases} z_1^* = \min : \lambda_1 \left| f_1 - z_1^* \right| \\ \\ z_2^* = \min : \lambda_2 \left| f_2 - z_2^* \right| \end{cases} \tag{4-34}$$

By minimizing the objective function presented in Eq. (4-33) based on a preferred weight vector, the scalar preferred solution will be a member of the optimum Pareto front. In this way, one can make sure that after introducing the preference (namely, the desired weight vector), an optimal trade-off will be conducted and the corresponding solution will be selected from the non-dominated Pareto solutions. The overall procedure of Tchebycheff optimization is schematically presented in Fig. 4-9.

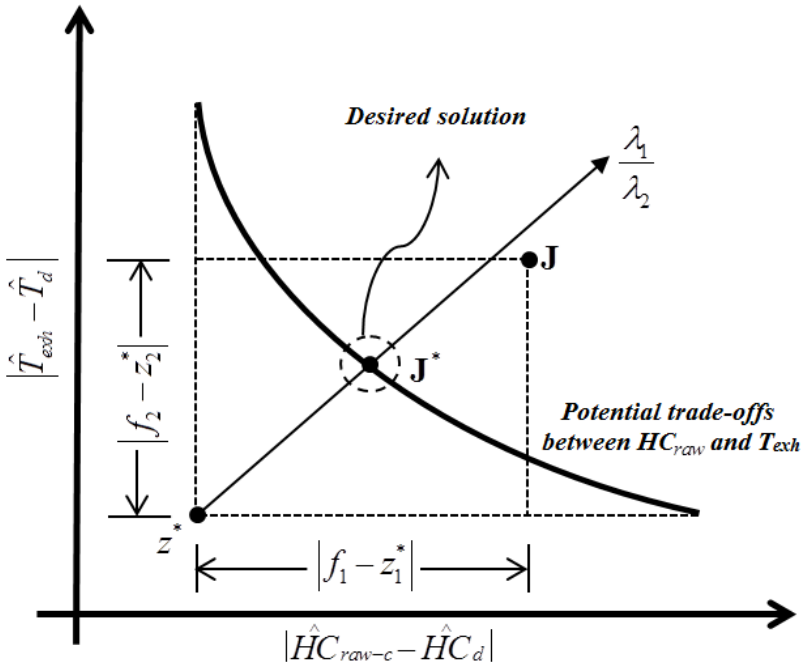

Figure 4-9 Schematic illustration of the Tchebycheff approach

The resulting non-smooth objective function is the only downside of the considered formulation. This means that solving the Tchebycheff-based problem by the means of gradient-based techniques,

for instance the steepest descent algorithm, may not provide the correct solution. However, we apply the above technique to the coldstart problem to form the objective function of PBNMPC controller. Let us write the objective function of coldstart problem as given below:

$$\mathbf{J} = \min : \sum_{i=1}^{H_P} \max \left\{ \lambda_1 \left\| \hat{HC}_{raw-c}\left(k+i\,|\,k\right) - \hat{HC}_d\left(k+i\,|\,k\right) \right\|^2 , \lambda_2 \left\| \hat{T}_{exh}\left(k+i\,|\,k\right) - \hat{T}_d\left(k+i\,|\,k\right) \right\|^2 \right\} \quad (4\text{-}35)$$

It can be seen that the both terms are formulated as minimization problems. This is because, the two terms present the distances of the values of $HC_{raw\text{-}c}$ and T_{exh} from the desired profiles (HC_d and T_d), instead of the minimization of $HC_{raw\text{-}c}$ and the maximization of T_{exh}. By defining certain values of the weights, the above scalar objective function can converge to a preferred non-dominated solution. However, there is one critical issue which should be verified. It is important to find out which pair of the weights can afford an optimal solution which is best compatible with the underlying physics of the problem. In fact, it should be verified that the control commands should be in favor of decreasing $HC_{raw\text{-}c}$ or increasing T_{exh}. To find out the characteristic of the desired solution, a primary test is conducted. In this way, the single version of the objective function with three sets of the weights is considered and an offline control algorithm is used to investigate the impact of each scenario on the quality of the final solution. The single version of the objective function and the three pairs of the weights are given below:

$$\mathbf{J} = \min : \sum_{i=1}^{H_P} \lambda_1 \left\| \hat{HC}_{raw-c}\left(k+i\,|\,k\right) - \hat{HC}_d\left(k+i\,|\,k\right) \right\|^2 + \lambda_2 \left\| \hat{T}_{exh}\left(k+i\,|\,k\right) - \hat{T}_d\left(k+i\,|\,k\right) \right\|^2 \quad (4\text{-}36)$$

$$\begin{cases} C_1 : \alpha = \lambda_1 / \lambda_2 = 0.80 \\ C_2 : \alpha = \lambda_1 / \lambda_2 = 1.00 \\ C_3 : \alpha = \lambda_1 / \lambda_2 = 1.25 \end{cases} \quad (4\text{-}37)$$

For the offline calculations, the desired profiles of the system outputs are calculated based on the following values of input signals [56]:

$$\begin{cases} HC_d : u_1 = 5\deg ATDC \;\; ; u_2 = 15.9 \\ T_d : \quad u_1 = 10\deg ATDC \; ; u_2 = 14.9 \end{cases} \quad (4\text{-}38)$$

The results of the sensitivity analysis indicate that by increasing the value of α from 0.8 to 1.25, the minimum of $HC_{raw\text{-}c}$ will be decreased (0.2423 g, 0.2357 g and 0.2257 g, respectively). This demonstrates the further importance of minimizing $HC_{raw\text{-}c}$, compared to the other term.

Based on the above analysis, the following objective function is considered for the PBNMPC controller:

$$\mathbf{J} = \min : \sum_{i=1}^{H_P} \max \left\{ 1.25 \left\| \hat{HC}_{raw-c}\left(k+i \mid k\right) - \hat{HC}_{d}\left(k+i \mid k\right) \right\|^2 , \left\| \hat{T}_{exh}\left(k+i \mid k\right) - \hat{T}_{d}\left(k+i \mid k\right) \right\|^2 \right\} \quad (4\text{-}39)$$

One of the remarkable advantages of the proposed PBNMPC scheme over other control algorithms lies in its capability to revise the desired profile in a real-time fashion based on the status of the system. In the offline calculations of the desired profiles, Eq. (4-38) is taken into account. However, these off-line calculations are performed regardless of the simplifications/assumptions used for the development of the coldstart model. Assume that under specific conditions, the engine system is inflicted in reality by some unknown and unpredictable disturbances or parameter variations. Therefore, the controller which is using the predefined desired trajectories provides improper commands, resulting in a poor performance with high HC_{cum}. If we can devise a policy to update the calculation of the desired profiles during the control process, it will enhance the performance of the controller in such conditions when there is a mismatch between the coldstart model and the real engine system behavior. The mentioned concept can be integrated with the PBNMPC strategy. In this context, at each updating point, the states of the first set point (k = 1) of the prediction horizon are replaced with the desired values of the states, and based on that, the prediction of the desired profile for the remaining set points (k = 2 to N) are performed using the input values reported in Eq. (4-38). Let us provide a mathematical definition for such a real-time desired profile builder. Suppose that the PBNMPC controller is at the beginning of one of its updating points and should predict the actual (Eq. (3-4)) and desired future states of the engine system. For the offline desired profile calculations, it only needs to put the values reported in Eq. (4-38) in Eq. (3-4). However, in the online optimum trajectory building scenario, the initial values (first set point) of the desired states are exactly the same as those used for the prediction of actual profile with using the feedback of the engine states. For the remaining set-points, the desired state values are predicted using the input signal variables given in Eq. (4-38). This can be mathematically expressed as given below:

$$\begin{cases} \begin{cases} x_1^d(k) = \delta t \cdot \dfrac{u_1(k-1)}{\tau_1} + \left(1 - \dfrac{\delta t \cdot k_1}{\tau_1}\right) x_1(k-1) \quad ; k = 2 \\ x_1^d(k) = \delta t \cdot \dfrac{60}{\tau_1} + \left(1 - \dfrac{\delta t \cdot k_1}{\tau_1}\right) x_1^d(k-1) \quad ; k = 3,...,N \end{cases} \\ \begin{cases} x_3^d(k) = \delta t \cdot \dfrac{16 - u_2(k-1)}{\tau_3} + \left(1 - \dfrac{\delta t \cdot k_3}{\tau_3}\right) x_3(k-1) \quad ; k = 2 \\ x_3^d(k) = \delta t \cdot \dfrac{16 - 14.9}{\tau_3} + \left(1 - \dfrac{\delta t \cdot k_3}{\tau_3}\right) x_3^d(k-1) \quad ; k = 3,...,N \end{cases} \end{cases} \tag{4-40}$$

$$T_d(k) = \max\left(x_1^d(k) + x_3^d(k), 0\right) + x_2(k) \tag{4-41}$$

$$\begin{cases} \begin{cases} x_5^d(k) = \delta t \cdot \dfrac{16 - u_2(k-1)}{\tau_5} + \left(1 - \dfrac{\delta t \cdot k_5}{\tau_5}\right) x_5(k-1) \quad ; k = 2 \\ x_5^d(k) = \delta t \cdot \dfrac{16 - 15.9}{\tau_5} + \left(1 - \dfrac{\delta t \cdot k_5}{\tau_5}\right) x_5^d(k-1) \quad ; k = 3,...,N \end{cases} \\ \begin{cases} x_6^d(k) = \delta t \cdot \dfrac{\left|u_1(k-1) - 55\right| + \left(u_1(k-1) - 55\right)}{2\tau_6} + \left(1 - \dfrac{\delta t \cdot k_6}{\tau_6}\right) x_6(k-1) \quad ; k = 2 \\ x_6^d(k) = \left(1 - \dfrac{\delta t \cdot k_6}{\tau_6}\right) x_6^d(k-1) \quad ; k = 3,...,N \end{cases} \end{cases} \tag{4-42}$$

$$HC_d(k) = \max\left(4000 - x_4(k), 800\right) + \max\left(x_5^d(k) + x_6^d(k), 0\right) \tag{4-43}$$

It should be noted that the states x_2 and x_4 depend on u_3 which is considered as a known input. Such real-time updating of the desired profiles are advantageous for the coldstart controller in practice where it is essential to track logical desired profiles to ensure proper HC_{cum} reductions.

In the next subsection, we scrutinize the algorithmic structure of MQFSA to explain how the non-smooth, non-convex objective function derived from the Tchebycheff analysis can be solved.

4.2.4 Multivariate quadratic fit-sectioning algorithm

To calculate the solution of objective function, here, a powerful non-derivative deterministic optimization algorithm is introduced which can be considered as a multi-dimensional version of the Brent's method [57]. MQFSA comprises of two different operators, namely the quadratic fitting and

golden sectioning mechanisms. MQFSA performs the optimization for each dimension independently, in a cooperative fashion. Firstly, we explain how the algorithm works (for one dimension), and then, extend the mechanism to fit the operators for multivariate problems.

Quadratic fitting mechanism: At the beginning of the procedure, a three-step pattern including points h_1, h_2, and h_3 is formed which satisfies the following criterion:

$$h_2 \in (h_1, h_3) \quad \Rightarrow \quad \mathbf{J}(h_1) < \mathbf{J}(h_2) < \mathbf{J}(h_3) \tag{4-44}$$

Thereafter, a quadratic polynomial is used to fit three points, which results in the following system of equations:

$$\begin{cases} \mathbf{J}(h_1) = a + bh_1 + ch_1^2 \\ \mathbf{J}(h_2) = a + bh_2 + ch_2^2 \\ \mathbf{J}(h_3) = a + bh_3 + ch_3^2 \end{cases} \tag{4-45}$$

Solving the equation below helps us to calculate the value of c:

$$c = \frac{1}{(h_3 - h_1)} \left(\frac{\mathbf{J}(h_1) - \mathbf{J}(h_2)}{h_2 - h_1} + \frac{\mathbf{J}(h_3) - \mathbf{J}(h_2)}{h_3 - h_2} \right) \tag{4-46}$$

Also, the minimum of **J** can be calculated by:

$$\mathbf{J}'(Q_t) = b + 2cQ_t = 0 \tag{4-47}$$

$$Q_t = \xi \left(\frac{h_1 + h_2}{2} \right) + (1 - \xi) \left(\frac{h_2 + h_3}{2} \right) \tag{4-48}$$

where:

$$\xi = \left(\frac{(h_2 - h_1)(\mathbf{J}(h_3) - \mathbf{J}(h_2))}{(h_2 - h_1)(\mathbf{J}(h_3) - \mathbf{J}(h_2)) + (h_3 - h_2)(\mathbf{J}(h_1) - \mathbf{J}(h_2))} \right) \tag{4-49}$$

We use the following operator to update the patterns:

$$\begin{cases} h_3 = Q_t \quad if \quad Q_t \in (h_2, h_3) \\ h_1 = Q_t \quad if \quad Q_t \in (h_1, h_2) \end{cases} \tag{4-50}$$

Let us consider that the optimum value at the current iteration is indicated by Q_t. At the next iteration, the optimum solution is known as Q_{t+1}. The current solution can be accepted if:

$$|Q_{t+1} - Q_t| < 0.5|h_2 - h_1| \tag{4-51}$$

Otherwise, the new solution Q_{t+1} is rejected and the golden sectioning algorithm is used to calculate Q_{t+1}.

Golden sectioning mechanism: This is a deterministic direct search strategy which uses a pre-defined bound (h_1, h_3) for the optimization. Here, two solutions are determined using the following formulation [57]:

$$\begin{cases} a = h_3 - \dfrac{h_3 - h_1}{1.6181} \\ b = h_1 + \dfrac{h_3 - h_1}{1.6181} \end{cases} \tag{4-52}$$

Then, based on that, Q_{t+1} is determined and the bounds are updated:

$$\begin{cases} \begin{cases} h_3 = a \\ Q_{t+1} = h_3 \end{cases} & if \quad \mathbf{J}(a) < \mathbf{J}(b) \\ \begin{cases} h_1 = b \\ Q_{t+1} = h_1 \end{cases} & if \quad \mathbf{J}(b) < \mathbf{J}(a) \end{cases} \tag{4-53}$$

Thereafter, the termination criterion (maximum iteration) is checked, and if it is not satisfied, the algorithm uses the criterion stated in Eq. (4-51) to select the proper operator. After termination of the criterion, the optimization through the first dimension is completed. This optimum value is stored at the vector of the solution and the same approach is used for the next dimension. Such a chain like mechanism is continued until all of the dimensions are exposed to MQFSA. The flowchart of MQFSA is given in Fig. 4-10. Based on the above definitions, the detailed block diagram of PBNMPC controller is presented in Fig. 4-11.

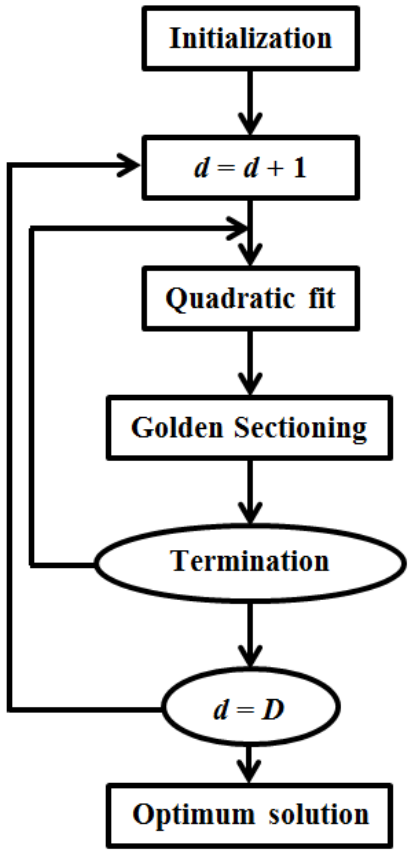

Figure 4-10 Flowchart of MQFSA

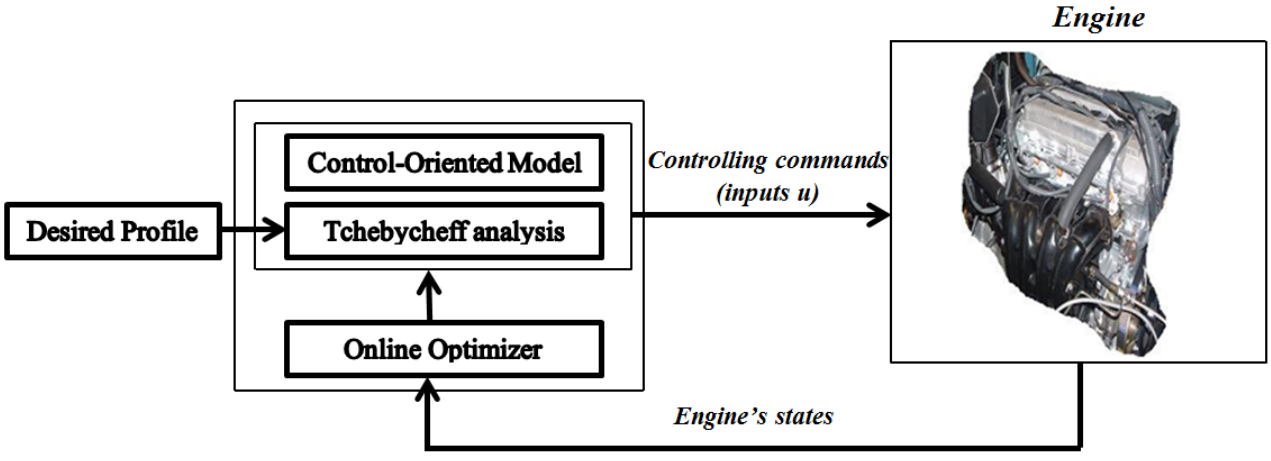

Fig 4-11 Block diagram of the PBNMPC controller

4.2.5 Parameter Settings and Simulation Setup

To conduct the simulations, the controller and some pre-defined profiles should be introduced. The controller consists of an optimizer and a control-oriented model. The detailed descriptions of the model and MQFSA were given previously. Other than MQFSA, the golden search (GS) algorithm is taken into account to check the efficacy of the proposed method for the PBNMPC calculations. Moreover, we use the standard nonlinear model predictive controller (NMPC) to further clarify the advantages of the proposed controller. The NMPC problem is optimized by sequential quadratic programming (SQP). It is worth noting that the both MQFSA and GS algorithms conduct the optimization within the range of unity, and also, the mapping to the real solution space is performed in the objective function. Based on this point, the extremes of each domain are taken as $a = 0$ and $b = 1$. To compare the performance of the proposed controller with a classical optimal controller, the Pontryagin's minimum principle (PMP) is considered. In our simulations, the engine speed profile ($u_3 = \varpi_e$) is a given external input and this is provided to the controller in the coldstart period. It is worth noting that for the development of NMPC and PBNMPC controllers, the prediction horizon length (H_P) of 2 *sec* is taken into account, and at each updating point, the horizon interval is divided into 15 set-points ($N = 15$).

The simulations are conducted under the three conditions used for the previous simulations. The computational facilities and encoding environments are exactly the same as those of the previous simulation.

4.2.6 Simulation Results

The simulation results can be categorized into four different parts. In the first part, we conduct a comparative study to demonstrate the efficiency of MQFSA for the optimization of the non-smooth objective function derived from Tchebycheff analysis. Thereafter, the effectiveness of PBNMPC approach is evaluated by repeating the simulations for 10 independent runs. At the third stage, statistical tests are provided to study the advantages of PBNMPC over the standard NMPC strategy with the conventional objective function. Finally, the performance of online PBNMPC controller is compared with the offline optimal controller derived from PMP.

To indicate the computational advantages of MQFSA over GS, a large-scale numerical benchmark problem, Rastrigin with D = 200, is taken into account. The result of the optimization procedure is depicted in Figure 4-12. The results clearly show that MQFSA has a much higher convergence speed compared to GS. Indeed, the computational effort of MQFSA is about 60% less than that for GS. Such a trait is especially advantageous for online applications as this is the case when MQFSA is incorporated into the PBNMPC controller. Figure 4-13 indicates the optimization performance of MQFSA of the PBNMPC controller for three sample updating points. It can be seen that the algorithm has a very good convergence behavior and it can neatly cope with the devised objective function.

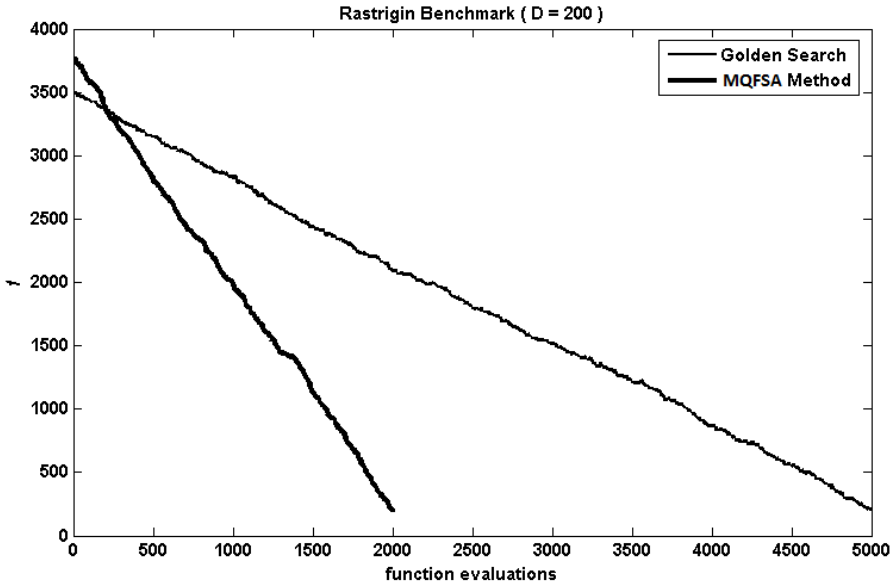

Figure 4-12 Comparison of GS and MQFSA for the large-scale Rastrigin benchmark

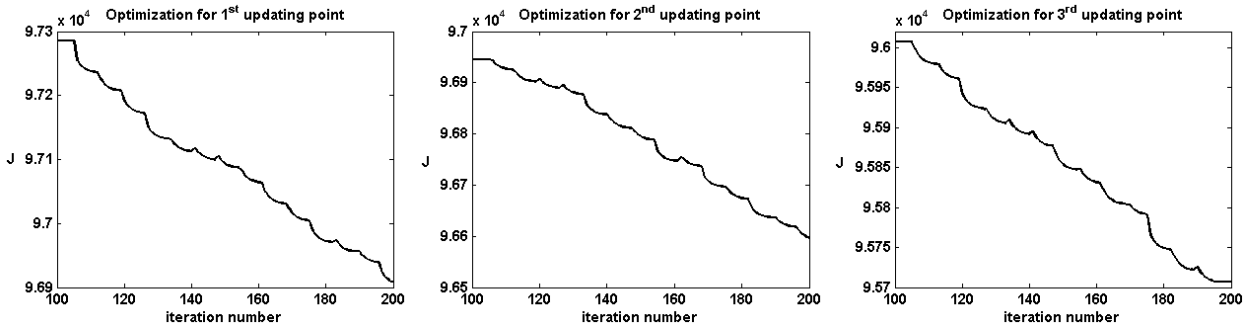

Figure 4-13 Optimization performance of MQFSA for three sample updating points of the PBNMPC controller

Table 4-6 Comparison between the performances of PBNMPC controllers with different online optimizers

Algorithms	*Case 1*		*Case 2*		*Case 3*	
	Calculation time	HC_{cum}	*Calculation time*	HC_{cum}	*Calculation time*	HC_{cum}
GS	0.043928	0.1623	0.044226	0.1753	0.048857	0.1773
MQFSA	0.046078	0.1530	0.046078	0.1574	0.051285	0.1623

Table 4-7 Performance of the PBNMPC controller over 10 independent runs

# Run	*Case 1*		*Case 2*		*Case 3*	
	Calculation time	HC_{cum}	*Calculation time*	HC_{cum}	*Calculation time*	HC_{cum}
1	0.046051	0.1525	0.046423	0.1577	0.051329	0.2241
2	0.046214	0.1536	0.046321	0.1573	0.051121	0.2254
3	0.046153	0.1533	0.046312	0.1574	0.051183	0.2125
4	0.046003	0.1523	0.046421	0.1571	0.051335	0.2142
5	0.046044	0.1537	0.046512	0.1574	0.051317	0.2111
6	0.046083	0.1535	0.046673	0.1573	0.051352	0.2143
7	0.046102	0.1521	0.046317	0.1577	0.051245	0.2310
8	0.046032	0.1522	0.046315	0.1575	0.051311	0.2112
9	0.046076	0.1528	0.046749	0.1570	0.051346	0.2142
10	0.046024	0.1537	0.046361	0.1577	0.051317	0.2155

Table 4-6 lists the results obtained by the PBNMPC controller with GS and MQFSA optimization algorithms. The results are presented in terms of the calculation time and HC_{cum}. It can be seen that the PBNMPC strategy with MQFSA can further reduce HC_{cum} in comparison with the PBNMPC scheme with GS optimizer. The other important observation pertains to the relatively similar computational time of the both optimizers, which, in turn, implies that MQFSA can efficiently be reconciled to the computational requirements of the PBNMPC controller. From a physical point of view, the performance evaluations of all controllers reveal that by imposing a higher engine speed, the value of HC_{cum} is decreased. Table 4-7 presents the results obtained by the PBNMPC controller over 10 independent runs. By taking a precise look at Table 4-7, it can be easily inferred that the obtained results are very similar. This, in turn, implies that the proposed PBNMPC approach is high-performance and has the capability of real-time implementations.

Figure 4-14 indicates the profiles spark timing obtained by the PBNMPC controller. It can be seen that the PBNMPC controller rapidly changes Δ from 5 BTDC deg. to 5 ATDC deg. (within 5 seconds), and after that, Δ gradually moves towards 10 ATDC deg. The variations of *AFR* are also indicated in Figure 4-15. It can be seen that the PBNMPC controller calculates the same profiles for

Case 2 and Case 3. In all of the cases, the PBNMPC controller has an inclination towards moving *AFR* to 16. Figure 4-16 indicates how the PBNMPC controller tries to increase the conversion efficiency of catalytic convertor. It can be seen that by increasing the engine speed, the PBNMPC controller can increase the efficiency of catalytic convertor in a shorter period of time. The time required for the PBNMPC controller to maximize the efficiency of catalytic convertor equals 22 *sec*, 26 *sec*, and 40 *sec*, for Case 1, 2, and 3, respectively. Figure 4-17 indicates T_{exh} profiles for the three cases. The obtained results indicate that by increasing the engine speed, more heat is provided to increase the catalyst temperature. Figure 4-18 illustrates the variations of HC_{raw} for the three considered cases. It can be seen that a pulse-type increase occurs at the very beginning of the process, and gradually, the emitted HC_{raw} converges to a constant value. The behavior of the engine revealed that this initial peak is necessary for reducing the risk of engine stalling. It can be seen that the convergence time of Case 1 is less than the other two cases. It can be also observed that the final value of HC_{raw} for Case 3 is more than the other cases. Figure 4-19 indicates the variations of engine-out (raw) *HC* emission rate (*g/s*). The rate variations are consistent with the changes of HC_{raw} shown in Figure 4-18. It can be seen that Case 1 reaches the zero emission rate in a shorter period of the time compared to the other cases. The obtained results indicate that by increasing the engine speed, the engine-out *HC* emission rate reduces to lower levels in a shorter period of the time. For further clarifying the performance of PBNMPC controller, the cumulative emitted *HC* profile is depicted in Figure 4-20. It can be easily seen that for Case 1, the emitted HC_{cum} is lower than the other two cases.

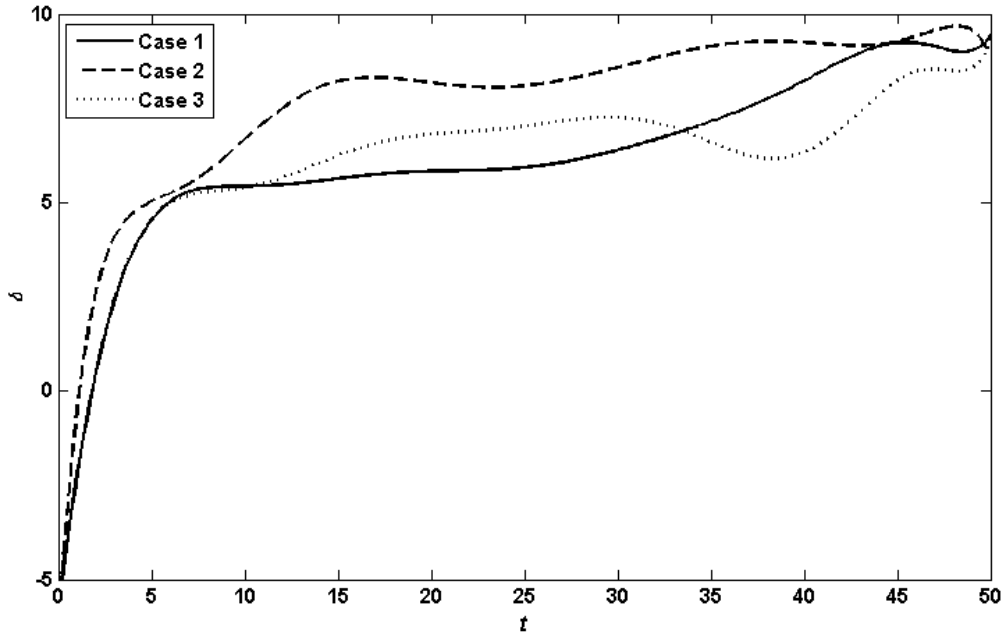

Figure 4-14 Calculated Δ profiles for the three considered cases

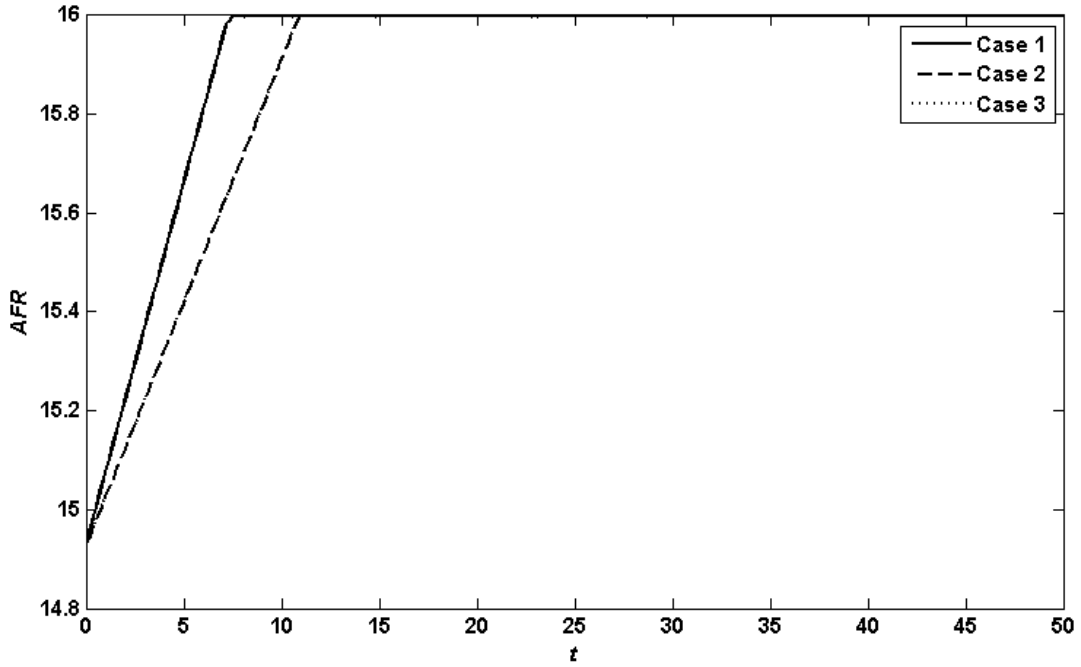

Figure 4-15 Calculated AFR profiles for the three considered cases

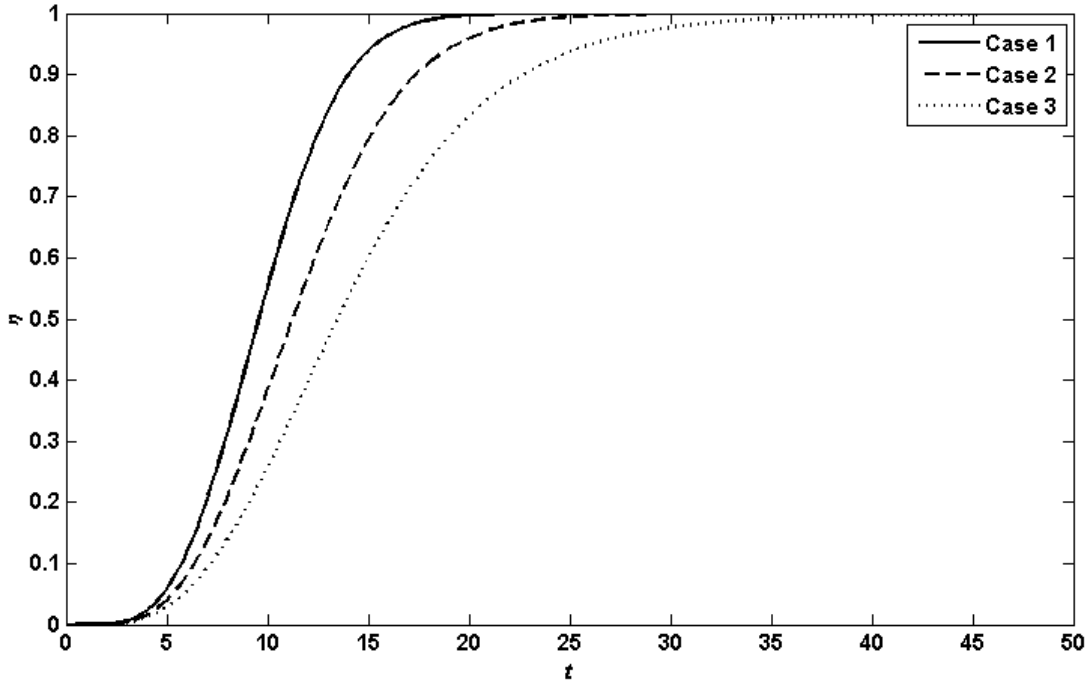

Figure 4-16 Catalyst efficiency for the optimum solutions

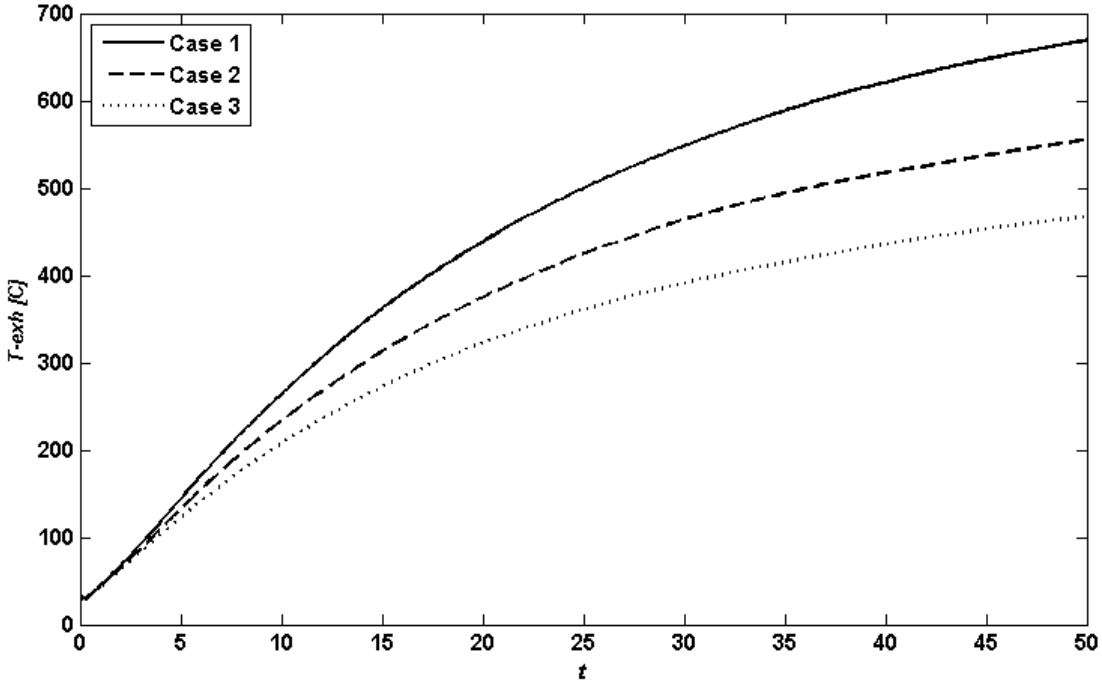

Figure 4-17 Optimum T_{exh} profiles obtained by the PBNMPC controller

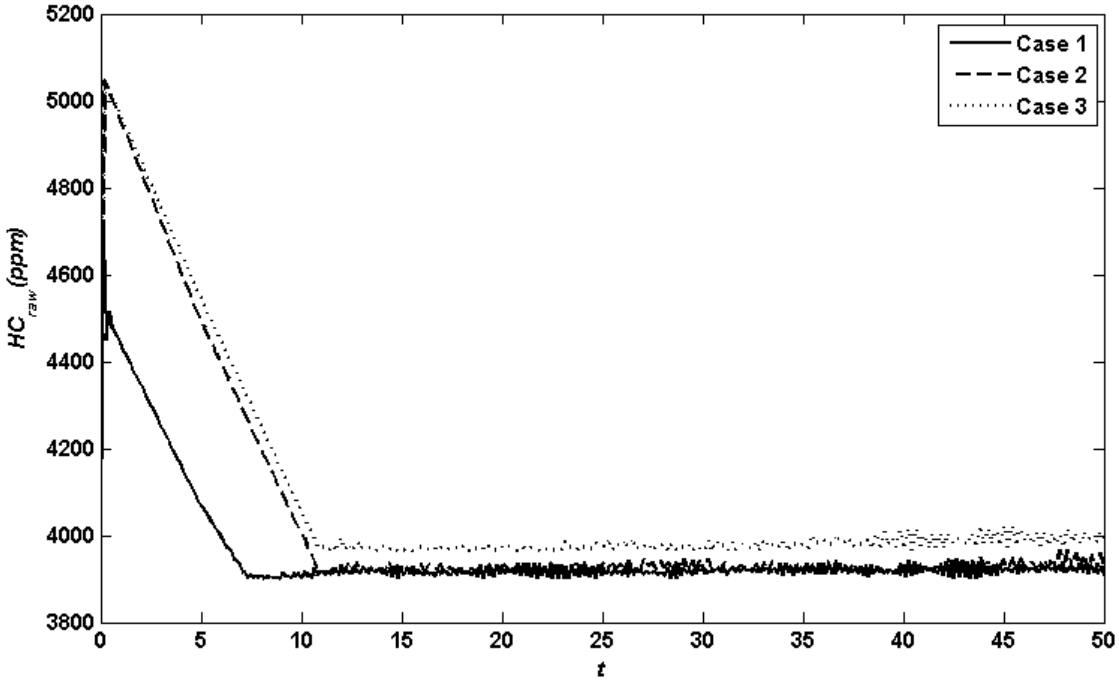

Figure 4-18 HC_{raw} profiles for the optimum solutions

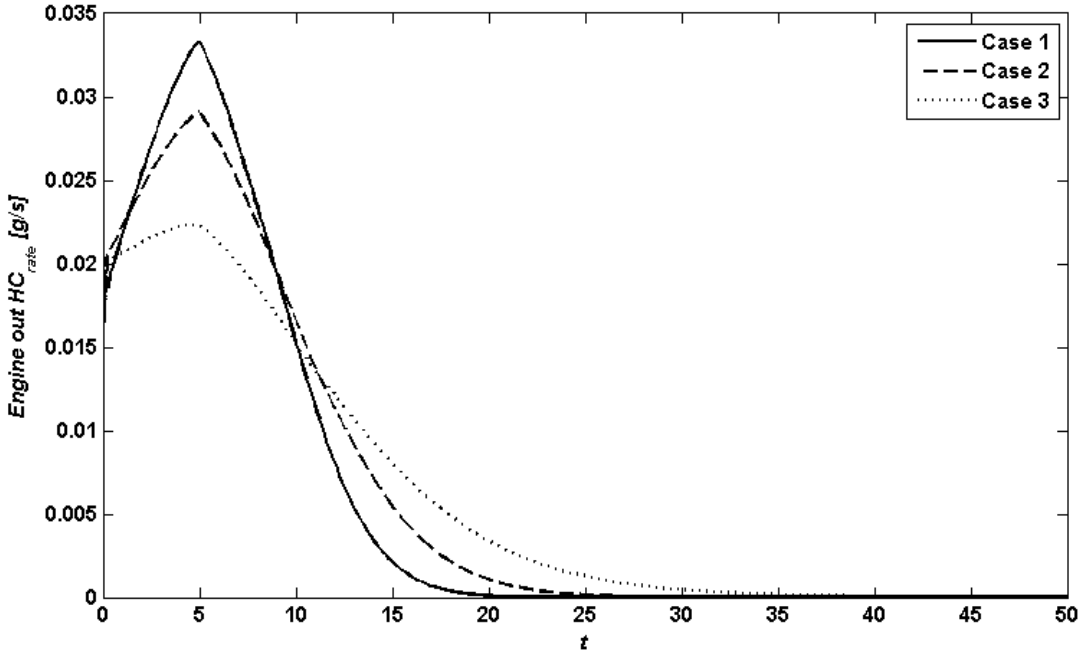

Figure 4-19 Engine-out (raw) *HC* emission rates for the optimum solutions

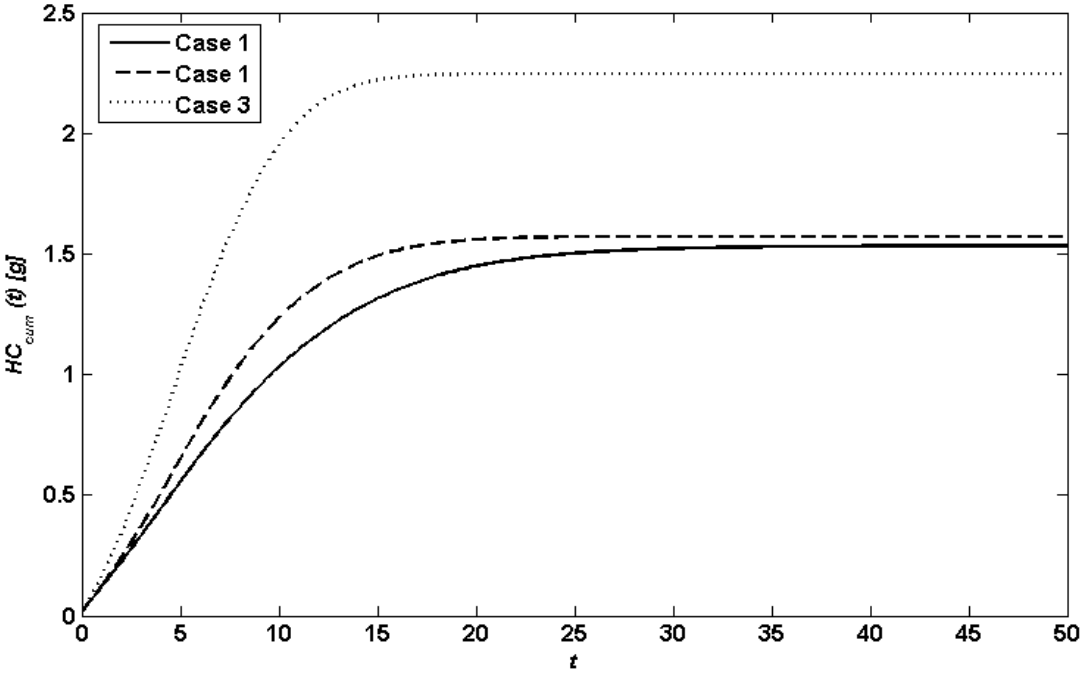

Figure 4-20 Cumulative HC_{cum} profiles for the three cases

At this stage of the numerical experiment, we compare the PBNMPC controller with the NMPC scheme derived by the classic objective function formulation to better demonstrate the efficacy of the proposed preference-based control approach for the considered case study. Table 4-8 lists the statistical results of PBNMPC and NMPC strategies for the three considered cases. The results demonstrate the superiority of PBNMPC over NMPC in terms of the both calculation time and performance. This is due to the efficiency of the Tchebycheff preference-based objective function at the heart of PBNMPC controller which not only reduces the complexity of the calculations, but also increases the functionality of the controller. The results indicate a significant difference between the performance of PBNMPC and NMPC controllers for Case 2 and Case 3. This clearly unveils the practical advantage of PBNMPC over NMPC.

In the final stage of the simulations, we would like to compare the performance of PBNMPC controller with the PMP technique. PMP is an open-loop optimal control scheme which is typically used for calculating the control commands offline, due to the significant computation time. However, it provides the global optimum solution. Table 4-9 compares the results obtained by the PBNMPC and PMP approaches. The results demonstrate the efficiency of the proposed PBNMPC controller. As it can be seen, the solutions provided by the PBNMPC technique are very close to those of PMP. Such an observation endorses the fact that PBNMPC can be reliably used for the coldstart control problem because it is not only capable of yielding the qualified solutions, but also can make decisions based on the feedback of the current states of the engine system, which makes it robust against the parameter uncertainties and unknown disturbances in practice.

The simulation results demonstrated the applicability of the proposed multivariate quadratic fit-sectioning algorithm (MQFSA) over GS for the optimization procedure. Furthermore, they revealed the efficacy of PBNMPC over the standard NMPC which utilizes the conventional coldstart objective function. By comparing the performance of PBNMPC and PMP controllers, it was indicated that the optimal solutions determined by PBNMPC are very close to those obtained through off-line PMP calculations. Such observations endorse the applicability of the proposed control method for reducing the emitted hydrocarbons over coldstart period in practice. Furthermore, based on the characteristics of the engine system, the proposed controller can take any type of the desired profiles and make a deliberate balance between HC_{raw} and T_{exh} to deliberately reduce HC_{cum} in the coldstart period.

Table 4-8 Statistical results for the PBNMPC and NMPC strategies

	# Run	*Case 1*		*Case 2*		*Case 3*	
		Calculation time	HC_{cum}	*Calculation time*	HC_{cum}	*Calculation time*	HC_{cum}
NMPC	*Best*	0.0608	0.2079	0.0646	0.2131	0.0729	0.2102
	Worst	0.0614	0.2207	0.0613	0.2280	0.0777	0.2358
	Mean	0.0612	0.2139	0.0618	0.2190	0.0748	0.2220
	Std.	5.3e-4	0.0050	0.0010	0.0051	0.0024	0.0080
PBNMPC	*Best*	0.046003	0.1521	0.046321	0.1570	0.051121	0.2111
	Worst	0.046214	0.1537	0.046749	0.1577	0.051352	0.2310
	Mean	0.046078	0.1530	0.046440	0.1574	0.051285	0.2173
	Std.	6.4349e-5	6.5836e-4	1.5746e-4	2.4698e-4	7.7650e-5	6.909e-3

Table 4-9 Results obtained by the PBNMPC and PMP techniques

Controller	*Case 1*	*Case 2*	*Case 3*
PMP	0.145	0.158	0.218
PBNMPC	0.153	0.157	0.217

4.3 Receding Horizon Sliding Controller (RHSC)

In this section, the general formulation of RHSC scheme is provided. The RHSC approach is a powerful discrete-time sliding controller proposed by Hansen and Hedrick [58]. The controller has proven to show stable results for highly nonlinear systems. Given the promising performance of RHSC technique, here, the streamline of investigations is extended and the method is applied to a challenging control problem, namely controlling the behavior of an SI engine over the coldstart periods.

4.3.1 Formulation of RHSC for Coldstart Problem

Assume that the state-space representation of a given nonlinear system can be mathematically expressed by:

$$\mathbf{X}(k+1)=\mathbf{f}\left(\mathbf{X}(k),\mathbf{U}(k),\phi_{\chi},k\right) \tag{4-54}$$

$$\mathbf{Y}(k)=\mathbf{h}\left(\mathbf{X}(k),\mathbf{U}(k),\phi_{y},k\right) \tag{4-55}$$

where ϕ_x and ϕ_y represent the matrix of internal parameters of the nonlinear model **f** and **h**, **X** represents the augmented form of the states of the system, **Y** shows the augmented form of the system outputs, and **U** shows the input matrix, as given below:

$$\mathbf{Y}(k)=\begin{bmatrix} y_1(k) \\ y_2(k) \\ \vdots \\ y_o(k) \end{bmatrix}; \quad \mathbf{X}(k)=\begin{bmatrix} x_1(k) \\ x_2(k) \\ \vdots \\ x_n(k) \end{bmatrix}; \quad \mathbf{U}(k)=\begin{bmatrix} u_1(k) \\ u_2(k) \\ \vdots \\ u_m(k) \end{bmatrix} \tag{4-56}$$

where *o*, *n* and *m* show the number of system's outputs, states and inputs, respectively.

By considering a difference operator *D*(.), a candidate for a discrete-time sliding variable can be expressed by:

$$s(k)=D(\varepsilon(k)) \tag{4-57}$$

where $\varepsilon(k)$ shows the tracking error between the outputs and the desired profiles, which can be mathematically shown by:

$$\varepsilon(k)=y(k)-y_d(k) \tag{4-58}$$

It is worth noting that for a multi-output system, the augmented form of *s* can be given by:

$$\mathbf{S}(k)=\begin{bmatrix} s_1(k) \\ s_2(k) \\ \vdots \\ s_o(k) \end{bmatrix} \tag{4-59}$$

The goal of RHSC scheme is to calculate the control commands such that *s* (*k*) be close to the reaching phase. Sarpturk et al. [59] demonstrated that a necessary and sufficient condition for a discrete-time sliding variable to reach the sliding phase is:

$$|s(k+1)|<|s(k)| \tag{4-60}$$

Hence, the control commands should be calculated such that the above criterion is satisfied. The RHSC controller is equipped with a kind of future information preview strategy that enables it make

decisions based on the behavior of the system over a future prediction horizon (H_P). Indeed, this is a common feature between the RHSC and MPC techniques which provides the resulting controller with an anticipatory behavior that has proven to be efficient for handling constraints on the system's states and inputs [60]. To equip the RHSC scheme with a predictive behavior, the vector of variable *s* over a prediction horizon is defined by:

$$\hat{\mathbf{S}}^* = \begin{bmatrix} \mathbf{S}(k|k) \\ \hat{\mathbf{S}}(k+1|k) \\ \vdots \\ \hat{\mathbf{S}}(k+N|k) \end{bmatrix} \tag{4-61}$$

where *N* shows the number of set points over a prediction horizon.

The same approach should be followed to form the receding horizon-based matrices for **U**, **X**, and **Y** as below:

$$\hat{\mathbf{U}}^* = \begin{bmatrix} \hat{\mathbf{U}}(k|k) \\ \hat{\mathbf{U}}(k+1|k) \\ \vdots \\ \hat{\mathbf{U}}(k+N|k) \end{bmatrix}; \quad \mathbf{X}^* = \begin{bmatrix} \mathbf{X}(k|k) \\ \hat{\mathbf{X}}(k+1|k) \\ \vdots \\ \hat{\mathbf{X}}(k+N|k) \end{bmatrix}; \quad \mathbf{Y}^* = \begin{bmatrix} \mathbf{Y}(k|k) \\ \hat{\mathbf{Y}}(k+1|k) \\ \vdots \\ \hat{\mathbf{Y}}(k+N|k) \end{bmatrix} \tag{4-62}$$

To calculate the control commands, an objective function should be defined. For the RHSC controller, reaching *s* of 0 is considered as the objective function to guarantee that it correctly tracks the desired profiles. Let us define the general form of the objective function of the RHSC scheme as given below:

$$\begin{aligned} &\min_{\mathbf{U}} \quad J(\mathbf{S}^*) \\ &s.t. \quad \mathbf{S}(i+1) = D(\varepsilon(i+1)), i = k,...,k+N \\ &\qquad \mathbf{X}(i+1) = \mathbf{f}(\mathbf{X}(i), \mathbf{U}(i)), i = k,...,k+N \\ &\qquad \mathbf{U}(i+1) \in [\mathbf{U}_i^{lb}, \mathbf{U}_i^{ub}], i = k,...,k+N \end{aligned} \tag{4-63}$$

The above objective function implies that the RHSC controller should decrease the deviations of the sliding variables from zero over a prediction horizon of length *N*. It is worth pointing out that the considered system is subject to some input variable constraints. Also, the above objective function should be solved at the each updating point for a given prediction horizon. To calculate the value of

objective function, three different approaches, namely l_1, l_2 and l_∞, can be taken into account. For example, l_1 norm objective can be obtained by the sum of absolute values of s over the considered prediction horizon. Also, l_2 norm objective is the square form of l_1. In addition, l_∞ norm objective is defined as the biggest absolute value of s within the prediction horizon. The mentioned objective functions can be mathematically expressed as:

$$\begin{cases} l_1\ norm: \quad J\left(\mathbf{S}^*\right)=\left\|\mathbf{S}^*\right\|_1 =\sum_{j=1}^{o}\sum_{i=k}^{k+N}\left|s_j\left(i+1\right)\right| \\ l_2\ norm: \quad J\left(\mathbf{S}^*\right)=\left\|\mathbf{S}^*\right\|_2 =\sqrt{\sum_{j=1}^{o}\sum_{i=k}^{k+N}s_j\left(i+1\right)^2} \\ l_\infty\ norm: \quad J\left(\mathbf{S}^*\right)=\left\|\mathbf{S}^*\right\|_\infty =\sum_{j=1}^{o}\left\{\max\left|s_j\left(i+1\right)\right|;\mathrm{i}=\mathrm{k},...,\mathrm{k}+\mathrm{N}\right\} \end{cases} \tag{4-64}$$

Each of the above forms of the objective functions has its own advantages and downsides, and therefore, it is necessary to check which of them can afford us the best control performance for the current case study. The above systems of equations form the general structure of the RHSC scheme. In the next subsection, we provide the detailed steps required for applying the RHSC approach to the coldstart problem.

4.3.2 Formulation of RHSC for Coldstart Problem

The formulations and descriptions of the input constraints are exactly the same of those defined for PBMPC, and for the sake of brevity, those repetitive definitions are not given here. However, the formulation of controller is specific, and thus, is given in detail in this subsection.

As mentioned previously, the engine system's state equations can be expressed by Eq. (3-4). It is obvious that to solve the state equations, some initial conditions are required. The initial values given in Eq. (4-24) are again considered to solve the control-oriented model equations. To calculate the time interval for the discrete-time model, the prediction horizon (H_P) and the number of set points (N) should be taken into account. Let us assume that the time interval is indicated by δt, then, Eq. (4-25) shows its relation with H_P and N.

In the previous studies on MPC-based controllers, it has been revealed that the value of the time interval has a direct impact on the efficiency of the control commands. Therefore, the above parameter should be optimally adjusted to ensure the RHSC controller works properly.

Let us define the augmented form of the system's output variables as given in Eq. (4-26). Also, let us consider the Euclidian distance as the standard difference operator:

$$s(k) = D(\varepsilon(k)) = \varepsilon(k) = \left|\mathbf{Y}(k) - \mathbf{Y}_d(k)\right| \tag{4-65}$$

By defining the desired values of the mentioned outputs, namely T_d and HC_d, the sliding variables required for the formation of RHSC controller can be defined as given below:

$$\mathbf{S}(k) = \begin{bmatrix} s_1(k) \\ s_2(k) \end{bmatrix} = \left|\mathbf{Y}(k) - \mathbf{Y}_d(k)\right| = \begin{bmatrix} \left|T_{exh}(k) - T_d(k)\right| \\ \left|HC_{raw-c}(k) - HC_d(k)\right| \end{bmatrix} \tag{4-66}$$

It is necessary to make sure that the following relation is valid for the sliding variables:

$$\mathbf{S}(k+1) < \mathbf{S}(k) \rightarrow \begin{bmatrix} \left|T_{exh}(k+1) - T_d(k+1)\right| \\ \left|HC_{raw-c}(k+1) - HC_d(k+1)\right| \end{bmatrix} < \begin{bmatrix} \left|T_{exh}(k) - T_d(k)\right| \\ \left|HC_{raw-c}(k) - HC_d(k)\right| \end{bmatrix} \tag{4-67}$$

Based on the formulation of the model given in Eq. (3-4), it can be inferred that the above criterion is a function of the system inputs (u).

Now, the general form of the objective function can be written, as follows:

$$\begin{aligned} \min_{\mathbf{U}} \quad & J(\mathbf{S}^*) \\ s.t. \quad & \mathbf{S}(i+1) = \left|\mathbf{Y}(i+1) - \mathbf{Y}_d(i+1)\right|, i = k,...,k+N \\ & \mathbf{S}(i+1) < \mathbf{S}(i) \quad , i = k,...,k+N \\ & \mathbf{U}(i+1) \in [\mathbf{U}_i^{lb}, \mathbf{U}_i^{ub}] \ , i = k,...,k+N \end{aligned} \tag{4-68}$$

The three standard forms of the objective function J can be given by:

$$\begin{cases} l_1\ norm: \quad J\left(\mathbf{S}^*\right)=\left\|\mathbf{S}^*\right\|_1=\sum_{i=k}^{k+N}\left|T_{exh}\left(i\right)-T_d\left(i\right)\right|+\left|HC_{raw-c}\left(i\right)-HC_d\left(i\right)\right| \\ l_2\ norm: \quad J\left(\mathbf{S}^*\right)=\left\|\mathbf{S}^*\right\|_2=\sqrt{\sum_{i=k}^{k+N}\left|T_{exh}\left(i\right)-T_d\left(i\right)\right|+\left|HC_{raw-c}\left(i\right)-HC_d\left(i\right)\right|} \\ l_\infty\ norm: \quad J\left(\mathbf{S}^*\right)=\left\|\mathbf{S}^*\right\|_\infty=\left\{\max\left|T_{exh}\left(i\right)-T_d\left(i\right)\right|+\max\left|HC_{raw-c}\left(i\right)-HC_d\left(i\right)\right|;\mathrm{i=k,...,k+N}\right\} \end{cases} \tag{4-69}$$

The resulting MPC controller has a quite simpler objective function compared to a nonlinear model predictive controller or NMPC controller for the coldstart problem. This is mainly due to the fact the NMPC formulation does not consider any sliding variable and just tries to minimize the value of HC_{cum}, as shown below:

$$J=\sum_{i=1}^{N}\left\|\left(1-\hat{\eta}\left(k+i\,|\,k\right)\right)\dot{m}_{exh}\left(k+i\,|\,k\right)\left(\frac{16}{28.5}\times10^{-6}\right)\hat{HC}_{raw-c}\left(k+i\,|\,k\right)\right\|_{Q(i)}^{2} \tag{4-70}$$

As it can be seen, the above equation involves the direct calculations of several variables. However, the control system's objective function is simplified to the tracking of desired profiles for the RHSC approach. Such a computational advantage is especially critical when the controller is used for real-time applications, for instance the coldstart control problem. It worth pointing out that the desired trajectories are obtained exactly the same as those defined for PBMPC.

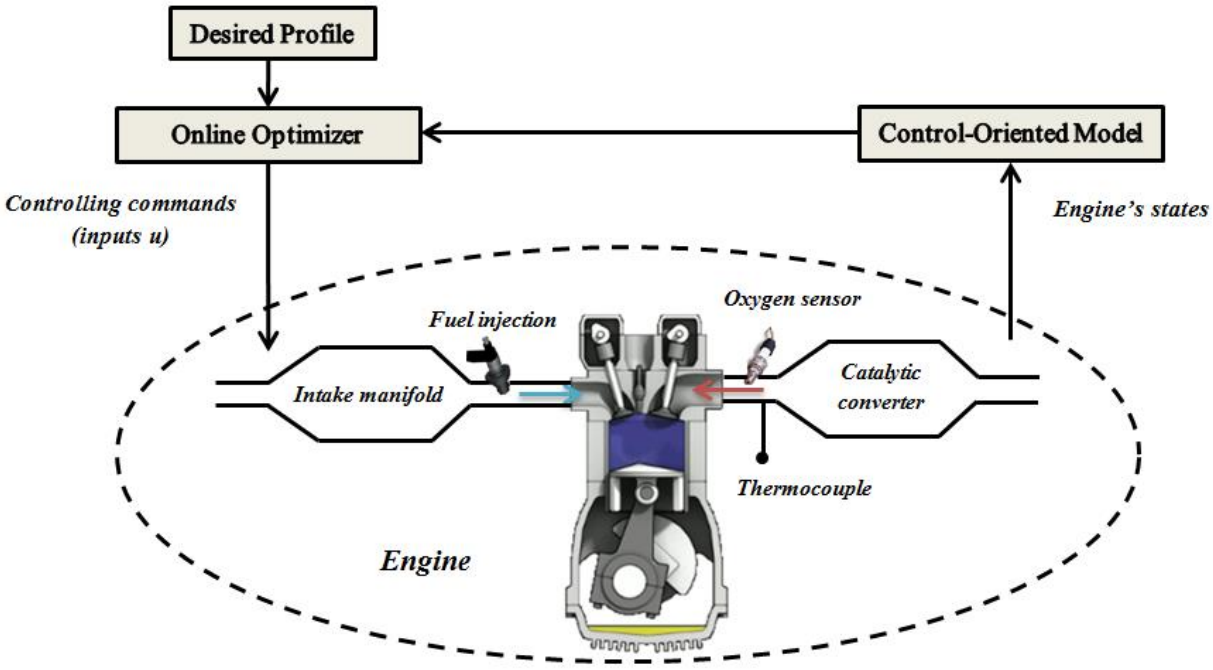

Figure 4-21 Schematic illustration of the RHSC scheme

Besides, MQFSA optimizer is used to calculate the optimal value of the objective function. A schematic illustration of the RHSC scheme is presented in Figure 4-21.

4.3.3 Parameter Settings and Simulation Setup

Prior to starting the simulations, some algorithmic parameters should be chosen. To evaluate the efficiency of the proposed RHSC controller NMPC is taken into account for comparison [13]. For the both NMPC and RHSC controllers, the prediction horizon (H_P) of 3 *sec* is considered, and in each horizon, 15 set-points (N) are taken into account. The sampling time is 0.2 *sec*. Also, to check the efficiency of MQFSA, a powerful non-derivative deterministic optimization technique, known as golden search (GS), is used. Both of the considered methods perform the optimization by normalizing the solution's bounds within the range of unity [0, 1]. Therefore, the bounds of the parameters a and b for the both MQFSA and GS are 0 and 1, respectively. It should be pointed out that to ensure the authenticity of the obtained results, the optimization and control of the engine system are conducted for 10 independent runs, and the statistical values, namely min, max, mean, and *std.* are reported. Moreover, to check the impact of different prediction horizons on the performance of the RHSC controller, we repeat the simulations for different values of H_P. The

considered values are 1, 2, 3, 4, 5, 6 *sec*. The performance of the controller is evaluated in terms of the computational complexity and accuracy to select the optimum value of H_P for the proposed predictive controller. In order to verify the potentials of RHSC approach for real-time implementations, the PMP-based controller is also taken into account. This is an open-loop optimal controller which calculates the control commands offline. To calculate the control commands based on the PMP approach, the steepest descent method is considered. The calculation of the input profiles by this method takes about 2 minutes. Although the solutions suggested by the PMP algorithm are global, it is not suited for the online implementations, and thus, it is necessary to have a faster control technique which can afford solutions close to PMP. The numerical experiments conducted in this study evaluate the accuracy of the RHSC scheme for the coldstart problem.

The simulations are conducted under the three conditions considered for the previous simulations. The computational facilities and encoding environments are also exactly the same as those of the previous simulations.

4.3.4 Simulation Results

To run the simulations, several aspects are taken into account. They include determining of the impact of the three forms of objective functions on the performance of RHSC scheme, evaluating the optimization power of MQFSA within the controller, comparing the performance of the RHSC and NMPC techniques, investigating the impact of different prediction horizons on the control performance, and finally, evaluating the real-time implementation potential of RHSC scheme by comparing it with the PMP approach.

Table 4-10 lists the statistical results obtained by the RHSC method for the three forms of objective functions over 10 independent runs. The main reason behind repeating the optimization procedure is that the optimization of the control objective is performed in a concurrent fashion for several times during the process. In this context, a slight deviation at a certain updating point deviates the optimization results of the upcoming updating points. Thus, it is necessary to conduct the optimization procedure for several independent runs to find out whether the final solution is the same.

Table 4-10 Performance of the RHSC scheme with different forms of objective functions over 10 independent runs

objective	*# Run*	*Case 1*		*Case 2*		*Case 3*	
		Calculation time	HC_{cum} (g)	*Calculation time*	HC_{cum} (g)	*Calculation time*	HC_{cum} (g)
l_1	*Best*	0.051222	0.1767	0.045634	0.1788	0.045216	0.1819
	Worst	0.051631	0.1770	0.047362	0.1791	0.047736	0.1822
	Mean	0.051377	0.1769	0.046489	0.1790	0.046517	0.1821
	Std.	1.29e-4	1.04e-4	5.47e-4	1.50e-4	9.22e-4	1.50e-4
l_2	*Best*	0.051220	0.1654	0.045634	0.1711	0.045637	0.1765
	Worst	0.051631	0.1654	0.046771	0.1711	0.047173	0.1765
	Mean	0.051394	0.1654	0.046321	0.1711	0.046259	0.1765
	Std.	1.50e-4	0	3.50e-4	0	3.99e-4	0
l_∞	*Best*	0.051143	0.1767	0.045634	0.1789	0.046104	0.1820
	Worst	0.051853	0.1770	0.046741	0.1791	0.046623	0.1822
	Mean	0.051473	0.1769	0.046285	0.1790	0.046241	0.1821
	Std.	2.15e-4	1.25e-4	3.10e-4	8.36e-5	1.46e-4	8.16e-5

It can be seen that all of the considered forms of objective functions can afford acceptable results for the coldstart problem. However, by taking a more precise look into the obtained results, it can be seen that the RHSC formulation with l_2-norm objective function shows better result, as compared to the other forms of the objective functions. Apparently, for all of the three cases, the RHSC scheme with the mentioned objective function reaches the *std.* value of 0 over 10 independent runs, which augurs its better performance. Furthermore, it can be observed that the mentioned controller can easily outperform the other variants of the RHSC for the same problem. It is also worth pointing out that the computational complexity of RHSC technique with each of the considered objective functions is in the same order. Considering the computational complexity and accuracy of RHSC approach with different forms of the objective functions brings us to the conclusion that the l_2-norm objective function can be an appropriate choice for the considered problem. Thus, in the rest of the simulations, it is used for the sake of comparative analysis.

After verifying the appropriate form of objective function for RHSC scheme, we evaluate the optimization power of MQFSA by comparing its performance to GS. The statistical results over 10 independent runs are reported in Table 4-11.

Table 4-11 Performance of the RHSC approach with different optimizers over 10 independent runs

# Run	*Case 1*		*Case 2*		*Case 3*	
	Calculation time	HC_{cumv} (g)	*Calculation time*	HC_{cum} (g)	*Calculation time*	HC_{cum} (g)
GS	0.047857	0.1667	0.043275	0.1755	0.043364	0.1791
MQFSA	0.051394	0.1654	0.046321	0.1711	0.046259	0.1765

Table 4-12 Performance of the RHSC method over 10 independent runs

# Run	Case 1		Case 2		Case 3	
	Calculation time	HC_{cum} (g)	Calculation time	HC_{cum} (g)	Calculation time	HC_{cum} (g)
1	0.051534	0.1654	0.046771	0.1711	0.046136	0.1765
2	0.051623	0.1654	0.046741	0.1711	0.046113	0.1765
3	0.051326	0.1654	0.045634	0.1711	0.046104	0.1765
4	0.051265	0.1654	0.046138	0.1711	0.046218	0.1765
5	0.051362	0.1654	0.046224	0.1711	0.046263	0.1765
6	0.051356	0.1654	0.046135	0.1711	0.046162	0.1765
7	0.051384	0.1654	0.046224	0.1711	0.046623	0.1765
8	0.051222	0.1654	0.046726	0.1711	0.045637	0.1765
9	0.051631	0.1654	0.046274	0.1711	0.046162	0.1765
10	0.051245	0.1654	0.046352	0.1711	0.047173	0.1765

The obtained results reveal that MQFSA can outperform GS. Furthermore, the computational time required for the calculation of the optimal solution is relatively the same for both of the considered algorithms. Such observations imply the fact that MQFSA can be a good choice for the RHSC scheme.

At this stage, we intend to compare the performance of NMPC and RHSC methods to find out the pros and cons of the proposed model-based predictive controller. To this aim, both of the controllers are applied to the engine system for 10 different runs. Tables 4-12 and 4-13 list the obtained results over 10 independent runs. The results reported in Table 4-12 clearly demonstrate that the RHSC scheme converges to the same solution. This augurs the high performance of RHSC approach, at least for controlling the considered engine over the coldstart period. By inspecting the results related to the NMPC method, it can be seen that the obtained solutions are not the same over independent runs. Furthermore, the results indicate that the computational complexity of NMPC method is higher than that of the RHSC technique. This is mainly due to the objective functions used inside the NMPC and RHSC controllers. As the objective function of RHSC method is simplified to the tracking a set of desired trajectories, the computational procedure required for the calculation of the control inputs are significantly less than that of the NMPC method. For more elaborations, the statistical results obtained for the NMPC and RHSC approaches over 10 independent runs are listed in Table 4-14. By throwing a glance at the obtained results, it can be easily found out that the RHSC approach outperforms the NMPC technique.

It is also necessary to investigate the impact different prediction horizons on the performance of RHSC approach. Table 4-15 lists the mean performance of the RHSC technique over 10

independent runs for different prediction horizon lengths. The results indicate that by increasing the prediction horizon length, the performance of RHSC controller is improved. However, there is a logical trade-off between the computational complexity of the controller and its accuracy. Indeed, by increasing the prediction horizon length of the controller, the computational complexity is increased, and at the same time, it accuracy is improved. As the RHSC controller is intended for real-time applications, we are not free to increase its computational complexity more than a certain threshold. For example, when the prediction horizon length is 5 or 6 *sec*, the final result is near to the global solution; however, the calculation time exceeds the time required for online calculations. By considering such criteria, H_P of 3 *sec* might be a logical choice for the current case study.

Table 4-13 Performance of the NMPC method over 10 independent runs

# Run	*Case 1*		*Case 2*		*Case 3*	
	Calculation time	HC_{cum} (g)	*Calculation time*	HC_{cum} (g)	*Calculation time*	HC_{cum} (g)
1	0.073467	0.2251	0.061424	0.2187	0.060549	0.2105
2	0.076564	0.2256	0.061812	0.2165	0.061322	0.2104
3	0.072929	0.2274	0.061333	0.2280	0.060835	0.2079
4	0.077763	0.2173	0.061463	0.2144	0.061500	0.2207
5	0.070773	0.2172	0.062092	0.2187	0.061337	0.2094
6	0.076469	0.2102	0.064675	0.2131	0.060856	0.2152
7	0.072382	0.2296	0.061416	0.2265	0.061416	0.2156
8	0.074392	0.2126	0.061337	0.2224	0.060329	0.2094
9	0.077670	0.2358	0.061322	0.2168	0.061416	0.2199
10	0.075762	0.2190	0.061506	0.2147	0.062150	0.2203

Table 4-14 Statistical results of the RHSC and NMPC methods over 10 independent runs

	# Run	*Case 1*		*Case 2*		*Case 3*	
		Calculation time	HC_{cum} (g)	*Calculation time*	HC_{cum} (g)	*Calculation time*	HC_{cum} (g)
RHSC	*Best*	0.051220	0.1654	0.045634	0.1711	0.045637	0.1765
	Worst	0.051631	0.1654	0.046771	0.1711	0.047173	0.1765
	Mean	0.051394	0.1654	0.046321	0.1711	0.046259	0.1765
	Std.	1.50e-4	0	3.50e-4	0	3.99e-4	0
NMPC	*Best*	0.0729	0.2079	0.0646	0.2131	0.0608	0.2102
	Worst	0.0777	0.2207	0.0613	0.2280	0.0614	0.2358
	Mean	0.0748	0.2139	0.0618	0.2190	0.0612	0.2220
	Std.	0.0024	0.0050	0.0010	0.0051	5.3e-4	0.0080

To evaluate the potential of RHSC scheme for real-time implementations, we compare its results to those of the PMP algorithm. As mentioned previously, the PMP method is a global optimal control technique, but requires significant computational efforts. This shortcoming of the PMP method can be taken care by the RHSC technique. The only thing which should be evaluated is to find out how much the reduction of emitted *HCs* for the RHSC technique is close to that of the PMP method. The results obtained by the RHSC and PMP approaches are listed in Table 4-16. The results demonstrate the high potential of RHSC method. As it can be seen, the values of HC_{cum} suggested by the RHSC controller are very close to those of the PMP technique. Furthermore, the time required for the RHSC calculations are significantly less than the PMP technique. Such observations indicate that the proposed controller has a good potential for automotive engine coldstart control applications. The devised RHSC controller is not only capable of yielding the qualified solution, but also can guide the output variables towards the desired profiles calculated online based on the feedback of the engine states. The real-time implementation potential of the RHSC method together with the entity of sliding controllers enable the RHSC technique to handle the deficiencies associated with parameter uncertainties and unknown disturbances observed in practice.

Table 4-15 Performance of the RHSC scheme for different prediction horizons over 10 independent runs

H_P (sec)	*Case 1*		*Case 2*		*Case 3*	
	Calculation time	HC_{cum} (g)	*Calculation time*	HC_{cum} (g)	*Calculation time*	HC_{cum} (g)
1	0.016473	0.1825	0.012746	0.1875	0.012645	0.1912
2	0.032464	0.1743	0.028958	0.1832	0.026453	0.1885
3	0.051394	0.1654	0.046321	0.1711	0.046259	0.1765
4	0.087536	0.1613	0.075745	0.1664	0.074342	0.1712
5	0.135734	0.1543	0.113457	0.1612	0.103745	0.1673
6	0.143653	0.1454	0.012365	0.1501	0.123485	0.1576

Table 4-16 HC_{cum} (g) obtained by the RHSC and PMP methods

Controller	*Case 1*	*Case 2*	*Case 3*
PMP	0.145	0.158	0.218
RHSC	0.1654	0.1711	0.1765

After evaluating the capability of RHSC scheme from different viewpoints, the physical behavior of automotive engine during the coldstart period should be investigated. The control signals calculated by the RHSC controller for the three considered cases are depicted in Fig. 4-22. It can be seen that the profiles of spark timing for the three cases have relatively the same shape. The spark timing changes rapidly from -5 deg. *ATDC* to 5 deg. *ATDC* within 5 seconds. Thereafter, it gradually increases from 5 deg. *ATDC* to 10 deg. *ATDC*. For *AFR*, a linear increase is suggested by the RHSC controller. It can be seen that the value of *AFR* increases from 14.9 to 15.03 within 50 seconds. The engine speed profiles for the three different cases are also indicated in the third section of Fig. 4-22. As mentioned previously, these profiles are known external inputs imposed on the system. It can be seen that the engine speed for *Case 1* is higher than *Case 2*, and the engine speed for *Case 2* is higher than *Case 3*. We analyze the outputs of the engine system based on these three cases.

Figure 4-23 indicates the shapes of T_{exh} profiles for the considered cases. As it can be seen, the final value of T_{exh} for *Case 1* is higher than that of *Case 2* and *Case 3*. It can be inferred that increasing the engine speed can directly increase the value of exhaust gas temperature. The final values of the exhaust gas temperature for the three cases are always confined within the range of 450 to 700 C.

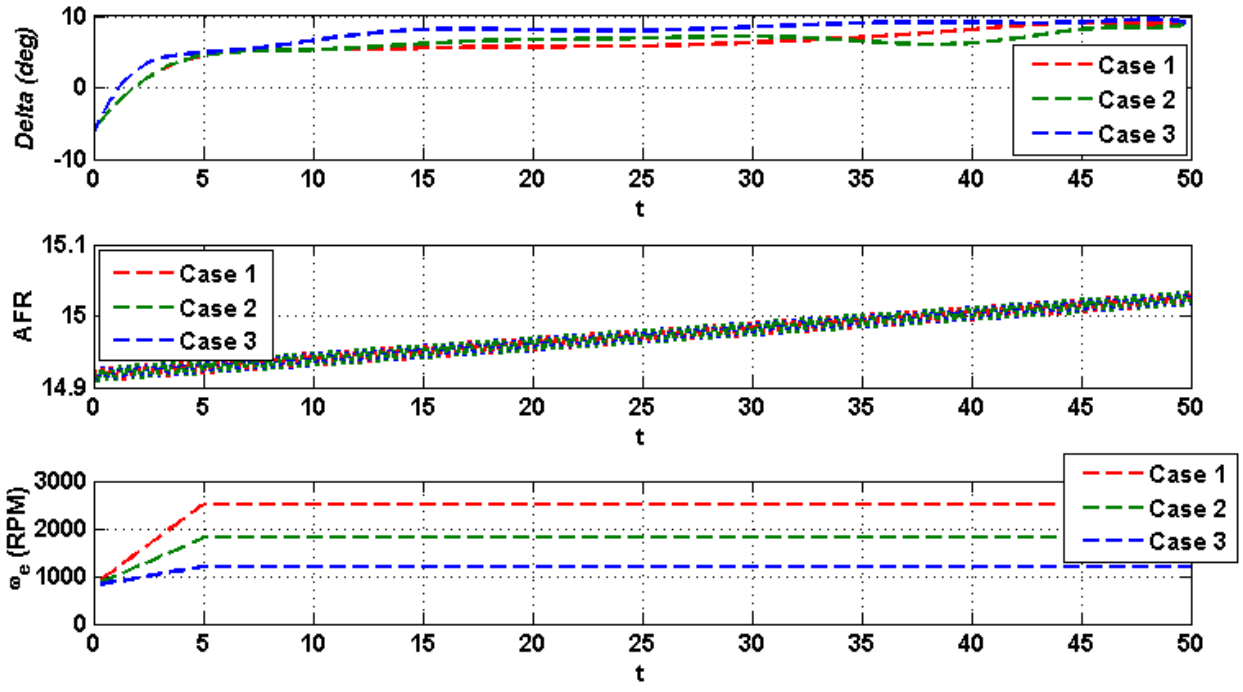

Figure 4-22 Control commands calculated by the RHSC controller

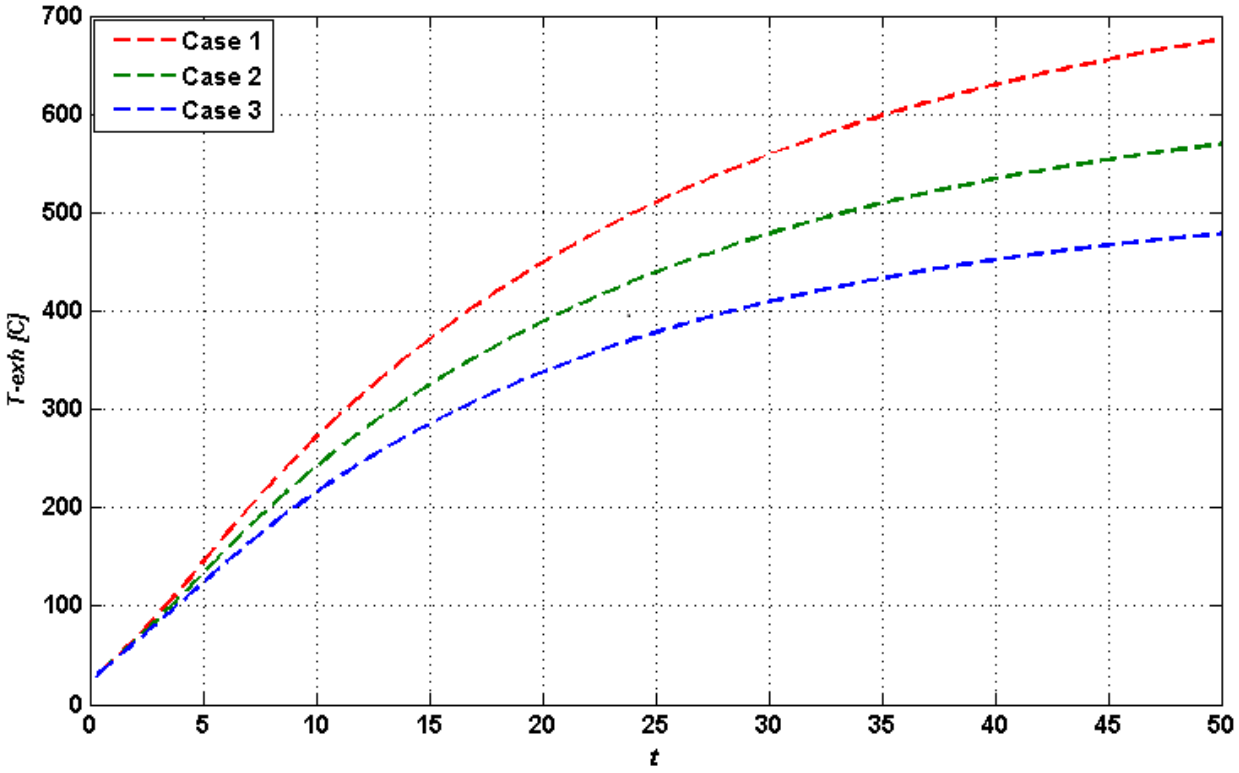

Figure 4-23 Optimum T_{exh} profiles obtained by the RHSC controller

The variations of engine-out HC_{rate} *[g/s]* for the three considered cases are illustrated in Fig. 4-24. A fast rise can be observed within the first 5 seconds of the control process, and after that, the emission rate starts to decrease until reaches the value of 0. The physical analysis revealed that the mentioned initial peak is necessary for reducing the risk of engine stalling. The obtained results indicate that the increase of HC_{rate} for *Case 1* is more than the other two cases, and also, the value of HC_{rate} for *Case 1* reaches 0 in a shorter period of time.

The conversion efficiency of the catalytic converter for the three considered cases can be seen in Fig. 4-25. As it can be inferred, increasing the engine speed helps the RHSC controller to increase the efficiency of the catalytic converter in a shorter period of time. The required time to maximize the efficiency of catalytic convertor equals 20 *sec*, 25 *sec*, and 35 *sec*, for *Case 1*, *2*, and *3*, respectively.

Figure 4-26 depicts the cumulative *HC* of the three considered cases. The final value of HC_{cum} for *Case 1* is less than the other two cases. This implies that HC_{cum} depends on the engine speed, and

also, increasing the engine speed decreases the final value of cumulative *HC* emissions over the coldstart period.

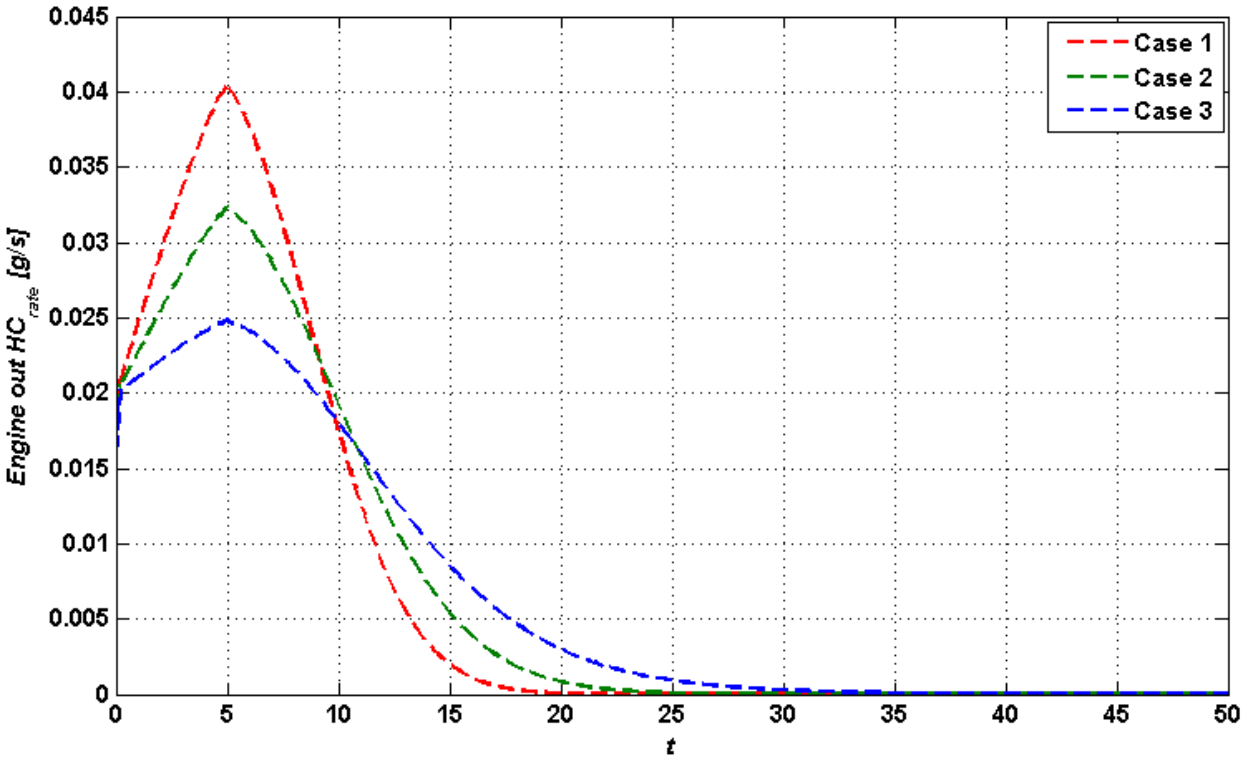

Figure 4-24 Engine-out *HC* emissions rate for the optimum solutions

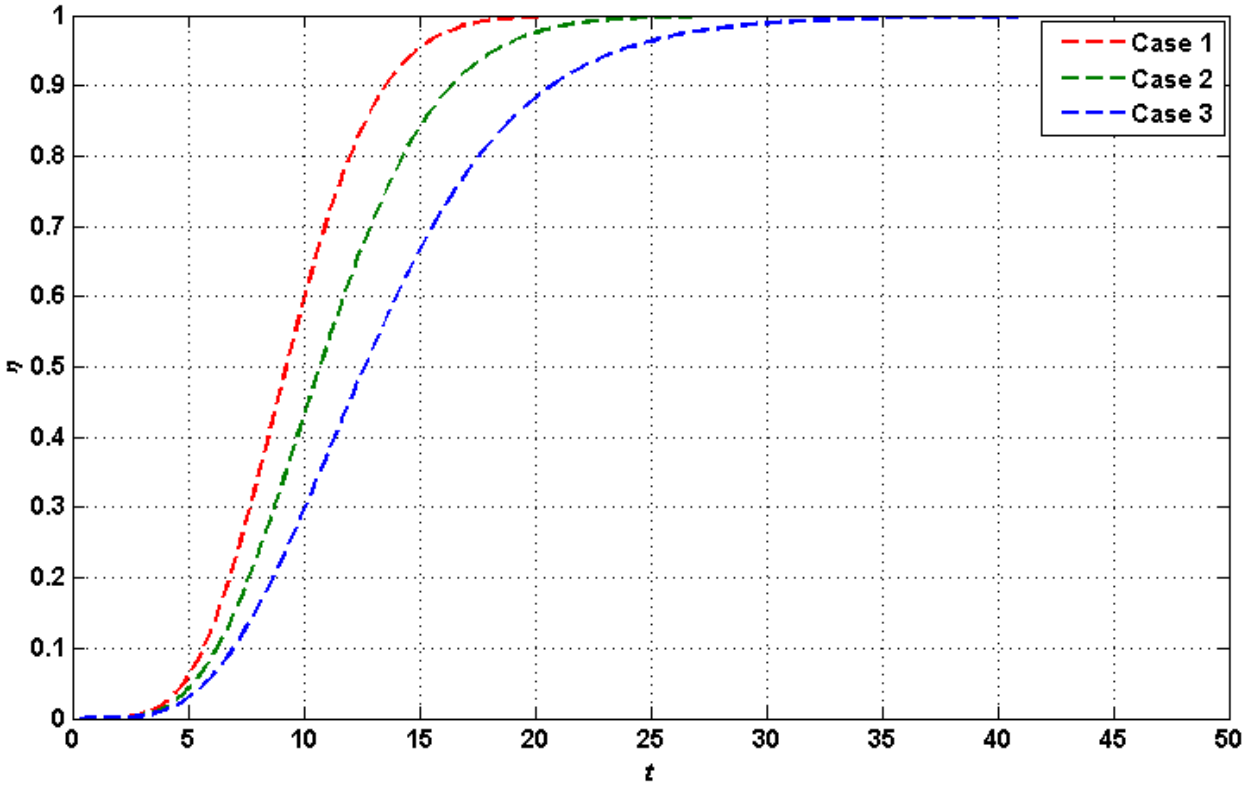

Figure 4-25 Catalyst efficiency for the optimum solutions

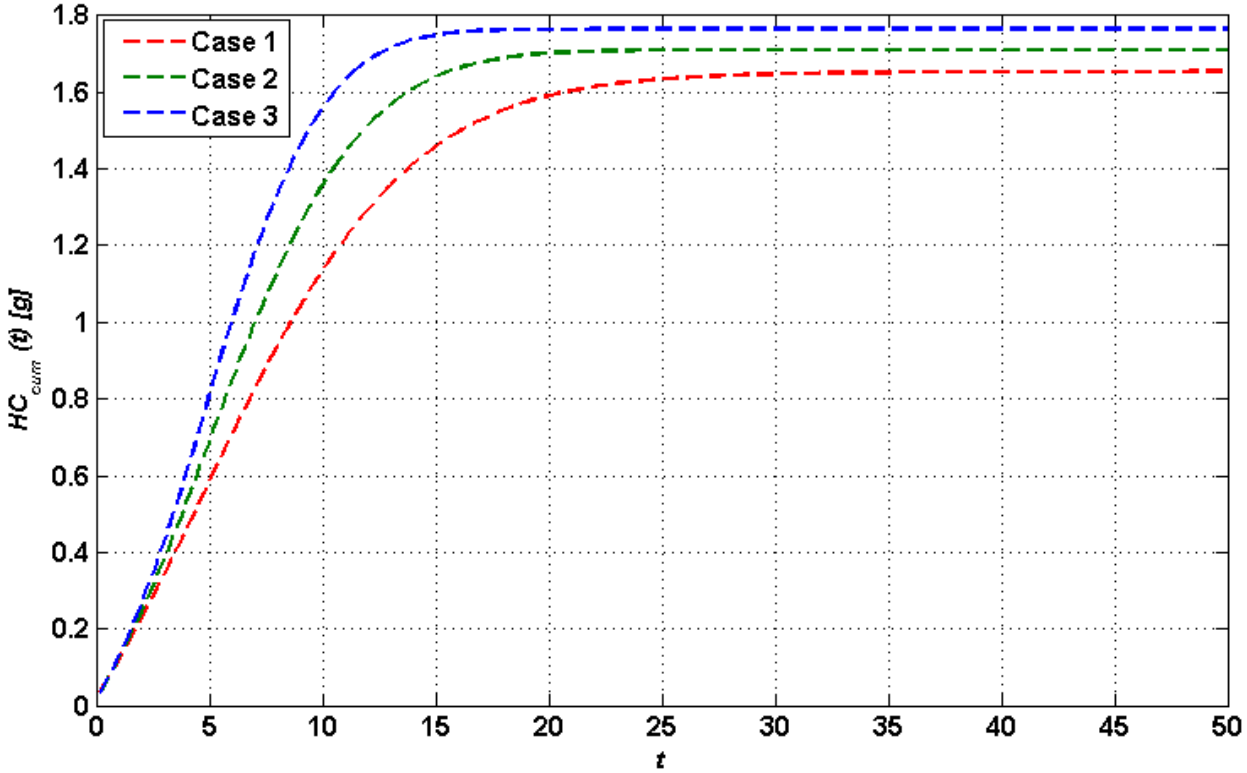

Figure 4-26 Cumulative hydrocarbon emission profiles for the three cases

4.4 Remarks on Using Predictive Strategies for Coldstart Control

By considering the results obtained by all of the devised predictive controlling strategies for the engine coldstart control problem, some seminal issues regarding the pros and cons of such techniques can be observed. As closed-loop controllers which operate based on the feedback of the real plant, predictive controlling strategies can provide a certain level of the robustness against the existing uncertainties and disturbances in practice, and it is expected that the calculated optimal control inputs be reliably used for controlling the behavior of engine. This is not the case when we are using open-loop optimal controllers, for instance PMP, which are based on the offline calculation of the controlling commands. One of the other aspects of the simulations carried out in this chapter lies in the fact that the considered predictive controllers have different types of objective functions and formulations, and thus, pursuing peculiar strategies for the control of engine performance.

In particular, NMPC was developed to solve the objective function resulting from the standard formulation of the coldstart controller, while PBNMPC was formulated to reach a desired trade-off between the conflicting objectives at the heart of coldstart control problem, and RHSC was designed to follow a set of the desired trajectories generated optimally in an online fashion. The results of the simulations demonstrated the effectiveness of the proposed predictive controllers with their specific solving procedures for real-time control applications. One of the main advantages of the proposed predictive strategies lies in their capability to handle different types of constraints in the formulation of control problem. Indeed, such a characteristic is often not the case when using different variants of optimal controllers available in the literature, and thus, the utilized predictive controllers benefit from this remarkable advantage.

However, as real-time controllers, there are some important issues concerning the implementation of the optimization module. To be more to the point, the optimizer at the heart of optimization module should be fast enough to result in a computationally-efficient controller suited for real-time applications, and on the other hand, the solver should be accurate enough to calculate the near-optimal controlling profiles to lead to a high-performance control. It is essential to take into account such considerations for practical applications.

Chapter 5

Conclusions and Future Work

This chapter is presented in two sections. In the first part, the conclusions resulting from the conducted simulations are presented. In the second section, some potential topics about the coldstart problem which are worth for further investigations are discussed to propose some future research directions in this area.

5.1 Conclusions

In this thesis, an extensive investigation was carried out to examine the potentials of predictive controlling strategies for managing the performance of automotive engines over the coldstart period to reduce the amount of cumulative tailpipe hydrocarbon emissions (HC_{cum}). In particular, two novel mode-based predictive controllers, namely receding horizon sliding controller (RHSC) and preference-based nonlinear model predictive controller (PBNMPC), and also a well-known predictive controller called nonlinear model predictive controller (NMPC) were taken into account for the simulations.

One of the contributions of this thesis lies in the proposition of an online optimum trajectory builder to optimally guide the controllers towards the desired trajectory. Also, different types of optimization methods together with powerful rival optimal controllers, e.g. Pontryagin's minimum principle (PMP), were used to further ascertain the veracity of the devised predictive controllers. Moreover, some novel optimization algorithms were proposed to obtain the optimum solutions in a very short period of time to make sure that the controllers can operate in a real-time fashion.

For NMPC, the simulations indicated that the devised dynamic particle swarm optimization (DPSO) can search the solution domain properly and yield an optimum solution in a very short period of time. By comparing the performance of DPSO with golden search (GS) and sequential quadratic programming (SQP), it was observed that the proposed DPSO can outperform those powerful rival methods, at least for the coldstart control problem. Furthermore, the results of the

simulations clearly demonstrated that NMPC can outperform well-known classical optimal controllers, for instance PMP.

The main motivation behind the proposition of PBMPC was the need for contriving a strategy for having a balance between the two conflicting objectives, i.e. minimizing the engine-out hydrocarbon emission ($HC_{raw\text{-}c}$) and maximizing the exhaust gas temperature (T_{exh}), at the heart of coldstart controller. The method involved solving the related optimization problem based on the Tchebycheff analysis technique, which enabled it to reach a balance between the two terms of the objective function. The results of simulations indicated that the resulting controller can optimally balance the conflicting objectives and reduces HC_{cum}. Furthermore, a modified searching algorithm, known as multivariate quadratic fit sectioning algorithm (MQFSA), was proposed to optimize the non-convex optimization problem resulting from the Tchebycheff analysis. By comparing the performance of MQFSA with GS and SQP, it was demonstrated that the proposed method is effective for the coldstart optimal control design.

Finally, the performance of RHSC was evaluated for the coldstart control problem. The simulation results indicated that combination of the sliding control and predictive control techniques can result in a very powerful controller suited for tracking the coldstart's desired trajectories in a real-time fashion while satisfying a set of the system constraints. Given the promising feedback of using MQFSA at the heart of PBMPC, the same optimization algorithm was used to calculate the optimal commands of RHSC. The results of simulations indicated that the proposed controller can outperform NMPC and PMP for the coldstart control problem.

To sum up, this investigation resulted in the following contributions:

- Examining the potential of different variants of model-based predictive control strategies for automotive engines HC_{cum} reduction over the coldstart period.
- Evaluating the performances of several novel techniques for solving the nonlinear optimization problems at the heart of proposed optimal controllers, and verifying their performances through different comparative analyses.
- Proposition of a novel online optimum trajectory builder to assist the coldstart controllers perform based on an optimum trajectory to further improve the engine performance.

- Suggestion of novel formulations for the objective functions to achieve high-performance predictive coldstart controllers.

5.2 Future Work

Based on the simulations carried out in this thesis, as well as detailed contemplations into the reports of the other active research groups in this area, we realized that there are still significant rooms for further investigations in the realm of automotive coldstart control design. In this context, the following remarks are provided as some research topics which are worth for future studies on the coldstart problem:

- Taking advantage of adaptive controllers, and also, an adaptable version of the used control-oriented model, to decrease the model/plant mismatch errors to boost the performances of devised predictive controllers.

- Seeking for more powerful analytical optimization algorithms for developing faster versions of the proposed predictive control strategies.

- Conducting a stability analysis to theoretically demonstrate that the devised controllers can yield a stable system when used in practice.

- Improving the structure of the presented controllers using stochastic operators to optimally deal with the undesired effects of noises, uncertainties, and disturbances in practice.

REFERENCES

[1] Rajmani R (2012) Vehicle dynamics and control. Mechanical Engineering Series, Springer-Verlag.

[2] Taghavipour A, Azad NL, McPhee J (2015) Real-time predictive control strategy for a plug-in hybrid electric powertrain. Mechatronics, doi:10.1016/j.mechatronics.2015.04.020.

[3] Ulsoy AG, Peng H, Cakmakci M (2014) Automotive control systems. Cambridge Press, Cambridge.

[4] Zhai YJ, Yu DL (2009) Neural network model-based automotive engine air/fuel ratio control and robustness evaluation. Eng Appl Artif Intell 22: 171–180.

[5] Taghavipour A, Azad NL, McPhee J (2012) An optimal power management strategy for power-split plug-in hybrid electric vehicles. Int J Veh Des 60(3/4): 286–304.

[6] Asadi B, Vahidi A (2011) Predictive cruise control: utilizing upcoming traffic signal information for improving fuel economy and reducing trip time. IEEE Trans Control Syst Technol 19(3): 707–714.

[7] Xiao L, Gao F (2010) A comprehensive review of the development of adaptive cruise control systems. Veh Syst Dyn 48(10): 1167-1192.

[8] Azad NL, Sanketi PR, Hedrick JK (2012) Determining model accuracy requirements for automotive engine coldstart hydrocarbon emissions control. J Dyn Syst - T ASME 134(5): 051002.

[9] Vajedi M, Azad NL (2014) Ecological adaptive cruise controller for plug-in hybrid electric vehicles using nonlinear model predictive control. IEEE Trans Intell Trans Syst, Accepted.

[10] Qin G, Ge A, Lee JJ (2006) Fuzzy logic control for automobiles I: knowledge-based gear position decision. Advances in Industrial Control, pp. 145-157.

[11] Chen X, Wang Y, Haskara I, Zhu G (2014) Optimal air-to-fuel ratio tracking control with adaptive biofuel content estimation for LNT regeneration, IEEE Trans Contr Sys Tech 22(2): 428-439.

[12] Cheng X, Jiang S, Wang S (2011) Design of a sliding mode controller for automotive engine speed regulation, IEEE Conference Industrial Electronics and Applications, Beijing, pp. 1722-1725.

[13] Mozaffari A, Vajedi M, Azad NL (2015) A robust safety-oriented autonomous cruise control scheme for electric vehicles based on model predictive control and online sequential extreme learning machine with a hyper-level fault tolerance-based supervisor, Neurocomputing 151(2): 845-856.

[14] Salehi R, Shahbakhti M, Hedrick JK (2014) Real-time hybrid switching control of automotive cold start hydrocarbon emission, J Dyn Syst - T ASME 136: 041002-1.

[15] Dextreit C, Kolmonovsky IV (2014) Game theory controller for hybrid electric vehicles, IEEE Trans Contr Sys Tech 22(2): 652-663.

[16] Azad NL, Khajepour A, McPhee J (2007) Robust state feedback stabilization of articulated steer vehicles, Vehicle Syst Dyn 45(3): 249-275.

[17] Zhang S, Zhang C, Han G, Wang Q (2014) Optimal Control Strategy Design Based on Dynamic Programming for a Dual-Motor Coupling-Propulsion System, Sci World J 2014: Article ID: 958239.

[18] Prokhorov DV (2008) Computational intelligence in automotive applications. Studies in Computational Intelligence, Springer-Verlag.

[19] Zavala JC (2007) Engine modeling and control for minimization of hydrocarbon coldstart emissions in SI engine, Ph.D. Thesis, University of California, Berkeley, USA.

[20] Sanketi PR, Zavala JC, Hedrick JK (2006) Automotive engine hybrid modeling and control for reduction of hydrocarbon emissions, Int J Control 79(5): 449-464.

[21] Wittka T, Muller V, Dittmann P, Pischinger S (2015) Development and investigation of diesel fuel reformer for LNT regeneration, Emiss Control Sci Technol doi:10.1007/s40825-015-0017-8.

[22] Brijesh P, Sreedhara S (2013) Exhaust emissions and its control methods in compression ignition engines: A review, Int J Auto Tech-Kor 14(2): 195-206.

[23] Shaw B, Hedrick JK (2003) Closed-loop engine coldstart control to reduce hydrocarbon emissions, American Control Conference 1392-1397.

[24] Sanketi PR, Zavala JC, Wilcutts M, Kaga T, Hedrick JK (2007) MIMO control for automotive coldstart. Fifth IFAC Symposium on Advances in Automotive Control, August.

[25] Zavala JC, Sanketi PR, Wilcutts M, Kaga T, Hedrick JK (2007) Simplified models of engine HC emissions, exhaust temperature and catalyst temperature for automotive coldstart, Fifth IFAC Symposium on Advances in Automotive Control, August.

[26] Mozaffari A, Azad NL, Hedrick JK (2015) A nonlinear model predictive controller for automotive coldstart hydrocarbon emissions reduction, IEEE Trans Vehicular Technology, Submitted.

[27] Henein NA, Tagomori MK, Yassine MK, Asmus TW, Thomas CP, Hartman PG (1995) Cycle-by-cycle analysis of HC emissions during cold start of gasoline engines, SAE Technical Paper, No. 952402.

[28] Dobner DJ (1983) Dynamic engine models for control development-Part I: Nonlinear and linear model formulation, Int J Vehicle Des 4: 54-74.

[29] Moskwa JJ, Hedrick JK (1987) Automotive engine modeling for real-time control applications, American Control Conference 341-346.

[30] Zavala JC, GAunther D, Sanketi PR, Willcutts M, Hedrick JK (2006) Fuel dynamics model for coldstart, Proceedings of ASME IMECE.

[31] Sanketi PR., Azad NL, Zavala C, Hedrick JK (2008) An optimal controller formulation via convex relaxation for automotive coldstart hydrocarbon reduction, 9th International Symposium on Advanced Vehicle Control 312-317.

[32] Shen H, Shamim T, Sengupta S (1999) An investigation of catalytic converter performances during cold starts, SAE Technical Paper, No. 1999-01-3473.

[33] Chan SH, Hoang DI (1999) Modeling of catalytic conversion of co/ch in gasoline exhaust at engine coldstart, SAE Technical Paper, No. 1999-01-0452.

[34] Fiengo G, Glielmo L, Santini S, Serra G (2002) Control of the exhaust gas emissions during the warm-up process of a TWC-equipped SI engine, 15th IFAC World Congress, Barcelona, Spain.

[35] Jones JP, Roberts JB, Pan J, Jackson RA (1999) Modeling the transient characteristics of a three way catalyst, SAE Technical Paper, No. 1999-01-0460.

[36] Jones JP, Roberts JB, Bernard P (2000) A simplified model for the dynamics of a three way catalytic convertor, SAE Technical Paper, No. 2000-01-0652.

[37] Koltsakis GC, Tsinoglou DN (2003) Thermal response of closed coupled catalysts during light-off, SAE Technical Paper, No. 2003-01-1876.

[38] Soumelidis M, Stobart R, Jackson R (2004) A nonlinear dynamic model for three-way catalyst control and diagnosis, SAE Technical Paper, No. 2004-01-1831.

[39] Gonatas E, Stobart R (2005) Prediction of gas concentrations in a three-way catalyst for on-board diagnostic applications, SAE Technical Paper, No. 2005-01-0054.

[40] McNicol AC, Figueroa-Rosas H, Brace CJ, Ward MC, Watson P, Ceen RV (2004) Coldstart emissions optimisation using an expert knowledge based calibration methodology, SAE Technical Paper, No. 2004-01-0139.

[41] Azad NL, Sanketi PR, Hedrick JK (2012) Sliding mode control with bounded inputs and its application to automotive coldstart emissions reduction, Invited Session on Advanced Control of Spark Ignited Engines, American Control Conference, Montreal, Canada.

[42] Amini MR, Shahbakhti M (2014) A novel singular perturbation technique for model-based control of cold start hydrocarbon emission, SAE International Journal of Engines, 7 (3), doi: 10.4271/2014-01-1547.

[43] Botsaris PN, Bechrakis D, Sparis PD (2003) An estimation of three-way catalyst performance using artificial neural networks during cold start, Appl Catal A Gen 243: 285-292.

[44] Mozaffari A, Azad NL (2014) Optimally pruned extreme learning machine with ensemble of regularization techniques and negative correlation penalty applied to automotive engine coldstart hydrocarbon emission identification, Neurocomputing 131: 143-156.

[45] Mozaffari A, Azad NL (2015) An ensemble neuro-fuzzy radial basis network with self-adaptive swarm based supervisor and negative correlation for modeling automotive engine coldstart hydrocarbon emissions: A soft solution to a crucial automotive problem, Appl Soft Comput 32: 449-467.

[46] Mozaffari A, Azad NL (2015) Coupling Gaussian generalised regression neural network and mutable smart bee algorithm to analyse the characteristics of automotive engine coldstart hydrocarbon emission, J Exp Theor Artif Intell 27(3): 253-272.

[47] Gray A, Ali M, Gao Y, Hedrick JK, Borelli F (2013) A unified approach to threat assessment and control for automotive active safety, IEEE T Intell Transp 14: 1490-1499.

[48] Kamal MAS, Mukai M, Murata J, Kawabe T (2013) Model predictive control of vehicles on urban roads for improved fuel economy, IEEE T Contr Syst T 21: 831-841.

[49] Maciejowski JM (2002) Predictive control with constraints. Prentice Hall.

[50] Yildiz ET, Farooqi Q, Anwar S, Chen Y, Izadian A (2012) Nonlinear constrained component optimization for the powertrain configuration of a plug-in hybrid electric vehicle powertrain, J Automotive Safety and Energy 3 (1): 64-70.

[51] Zou Q, Ji J, Zhang S, Shi M, Luo Y (2010) Model predictive control based on particle swarm optimization of greenhouse climate for saving energy consumption, Word Automation Congress 123-128.

[52] Karimi J, Nobahari H, Pourtakdoust SH (2012) A new hybrid approach for dynamic continuous optimization problems, Appl Soft Comput 12: 1158-1167.

[53] Kiefer J (1953) Sequntial minimax search for a maximum. Proc American Mathematics Society 4: 502-506.

[54] Borrelli F, Bemporad A, Fodor M, Hrovat D (2001) A hybrid approach to traction control, Hybrid Systems: Computation and Control (Lecture Notes in Computer Science), Vol. 2034, Springer, Berlin, 162-174.

[55] Sanketi PR (2009) Coldstart modeling and optimal control design for automotive SI engines, Ph.D. Thesis, University of California, Berkeley, USA.

[56] Azad NL (2015) A model-based scheme for on-line optimization of automotive coldstart hydrocarbon emission control strategy, Proc Inst Mech Eng I: J Syst Control Eng, In-Press.

[57] Chandrupatla TR (1998) An efficient quadratic fit-sectioning algorithm for minimization without derivatives, Comput Methods in Appl Mech Eng, 152: 211-217.

[58] Hansen A, Hedrick JK (2015) Introducing the concept of receding horizon sliding control for linear and nonlinear systems, American Control Conference.

[59] Sarpturk SZ, Istefanopulos Y, Kaynak O (1987) On the stability of discrete-time sliding mode control systems, IEEE T Automat Contr 32 (10): 930-932.

[60] Borrelli F (2003) Constrained optimal control of linear and hybrid systems, Springer.